Ductile roots of mature strike-slip faults: Integrating field and laboratory observations with numerical models

Yuri Fialko

Institute of Geophysics and Planetary Physics
Scripps Institution of Oceanography
University of California San Diego

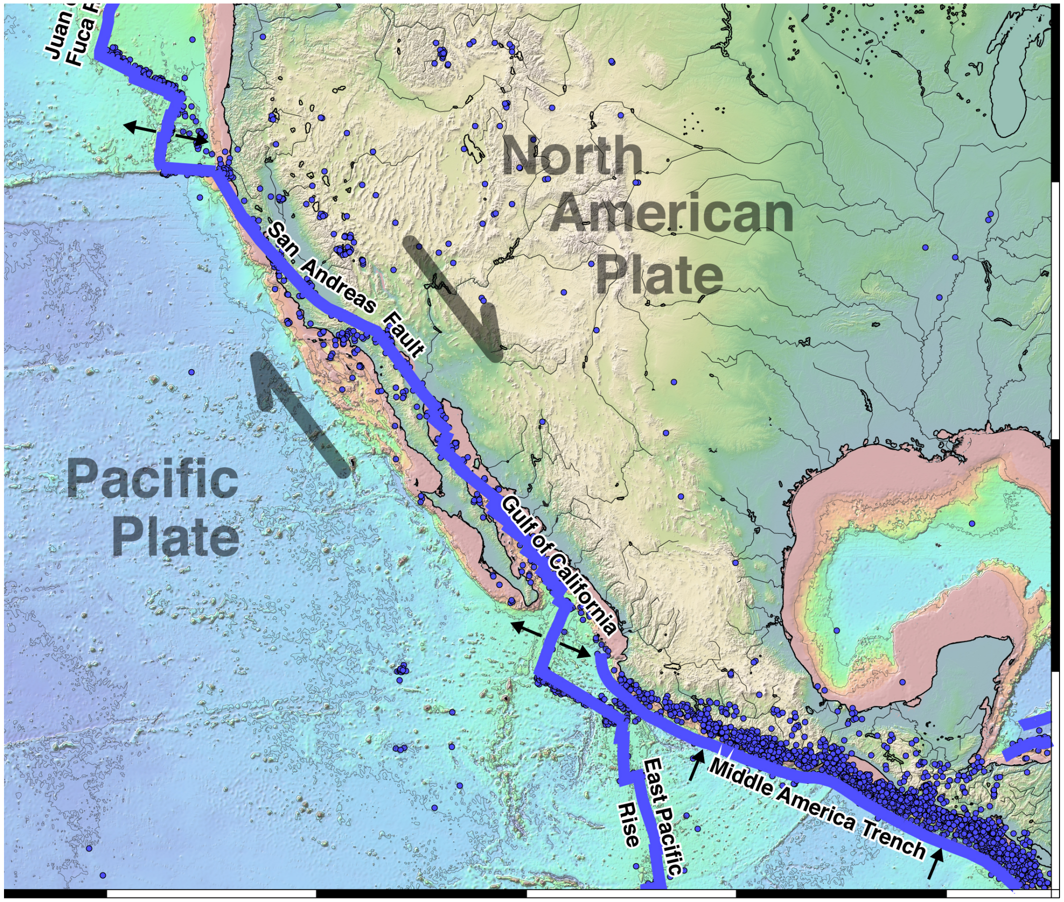
North American Plate
Pacific Plate
San Andreas Fault
Gulf of California
Middle America Trench
East Pacific Rise


SAF, Carrizo plains

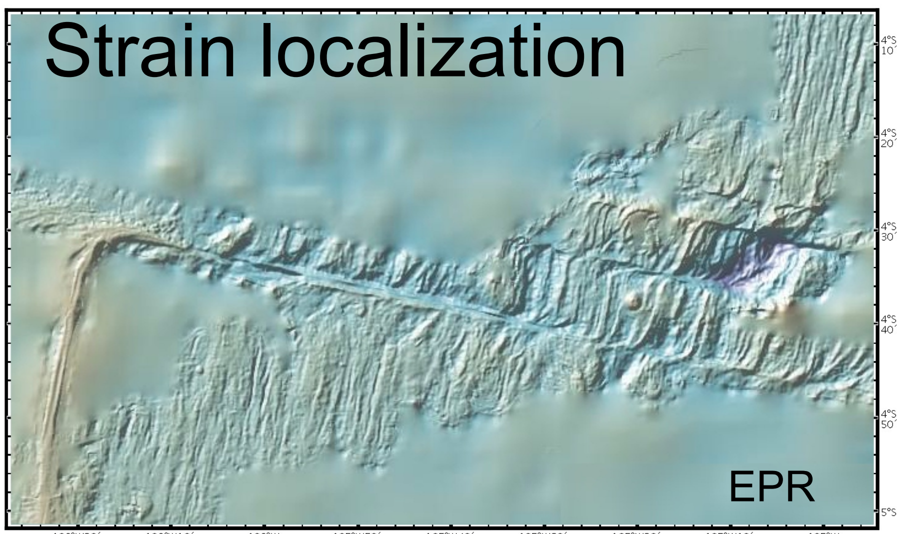
Strain localization
EPR

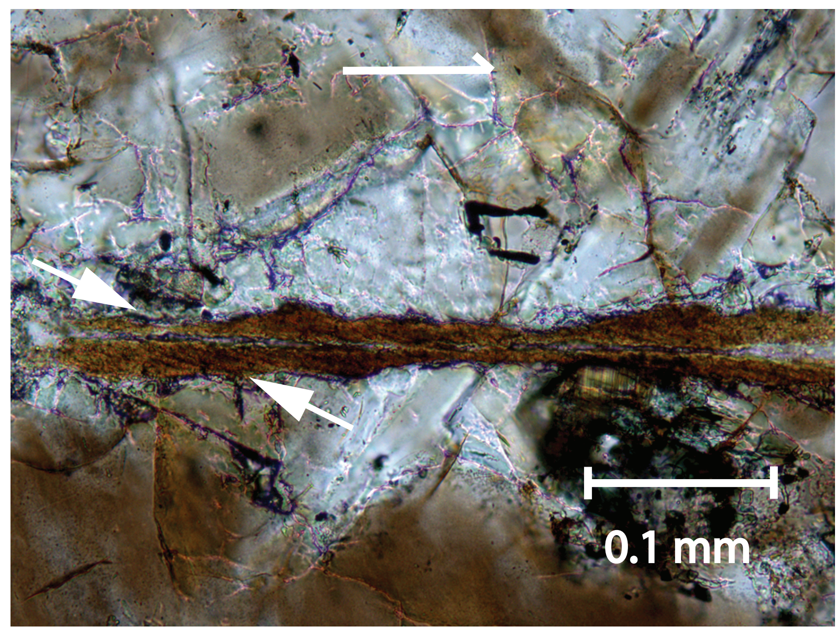
0.1 mm

Field geology & laboratory view of a major crustal fault

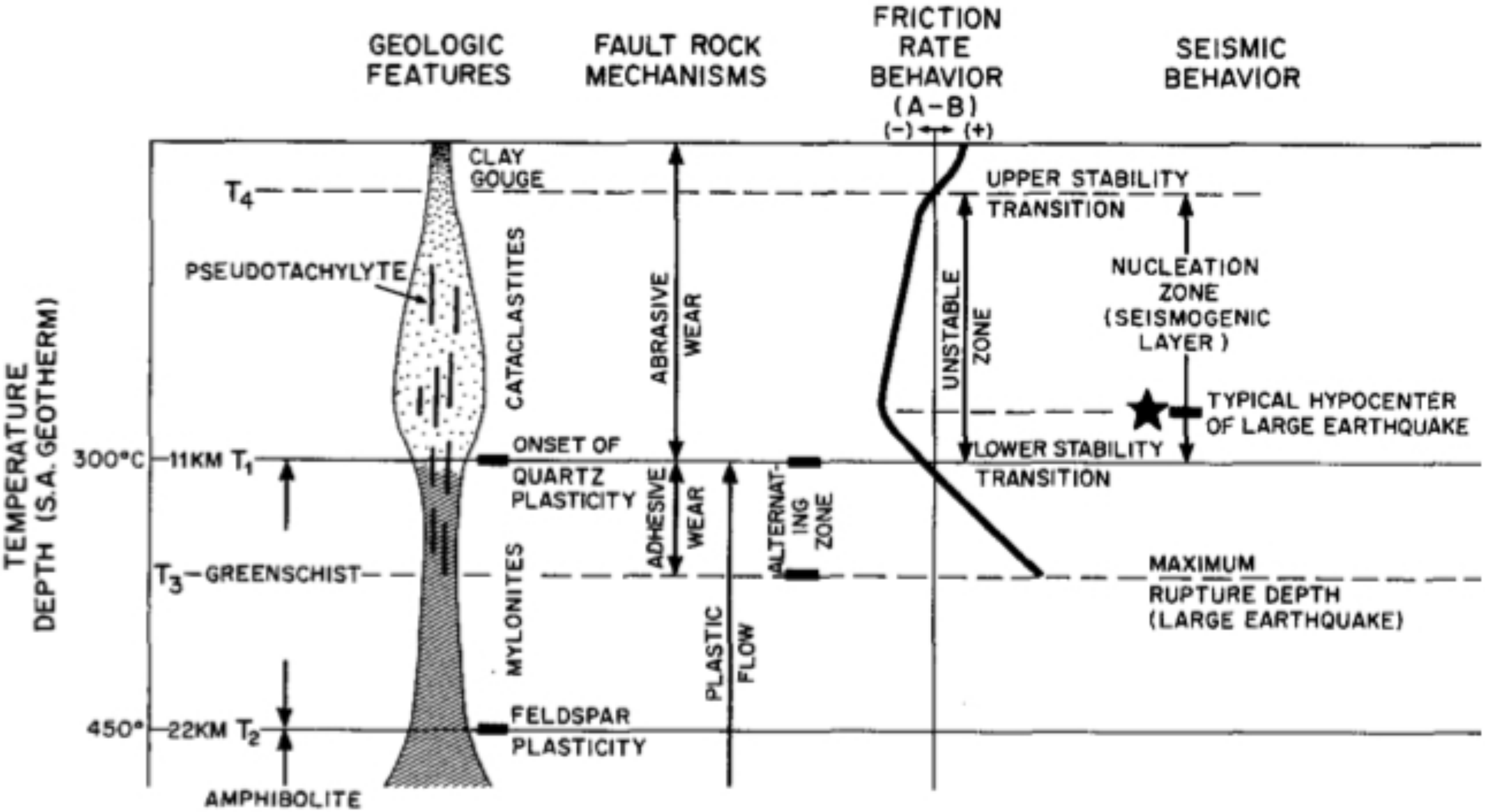

Scholz, 1988

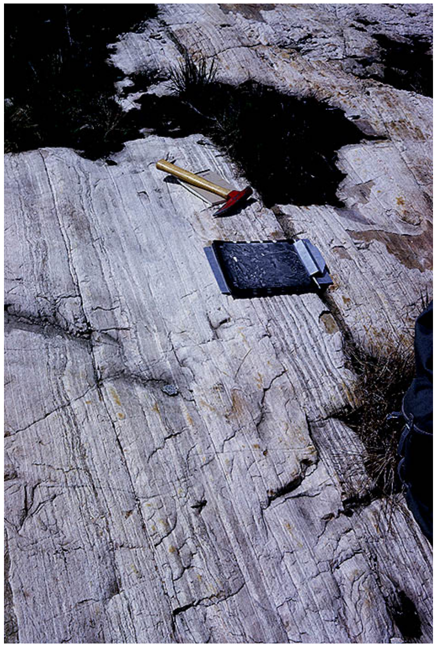

Mylonite zone (Ontario, Canada)

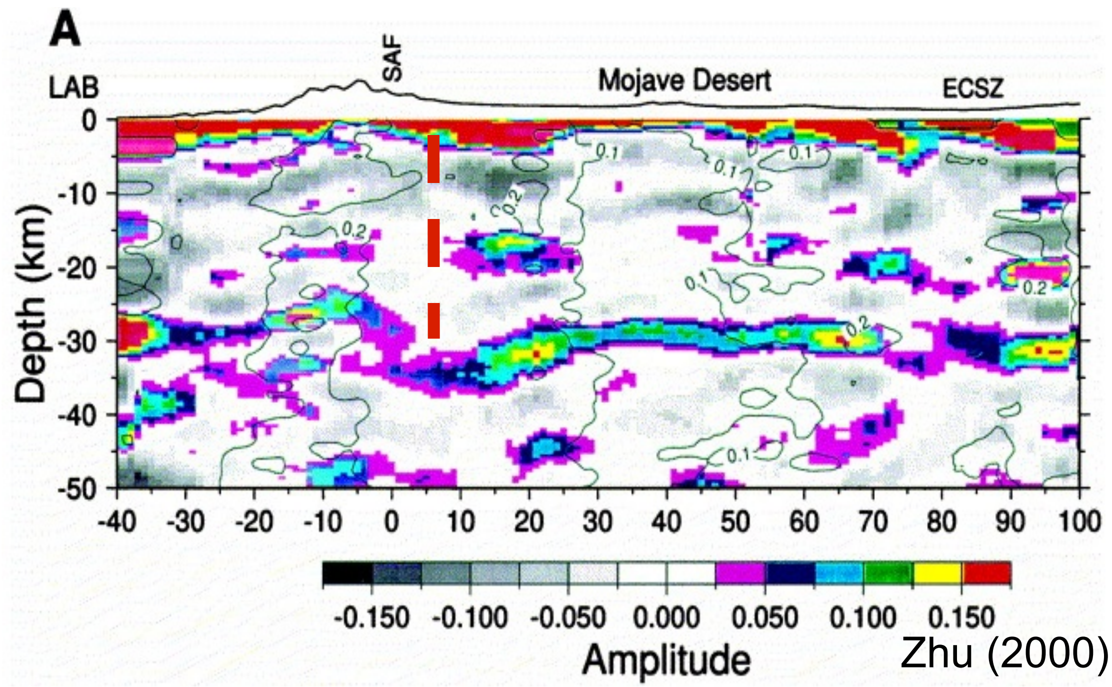

Zhu (2000)

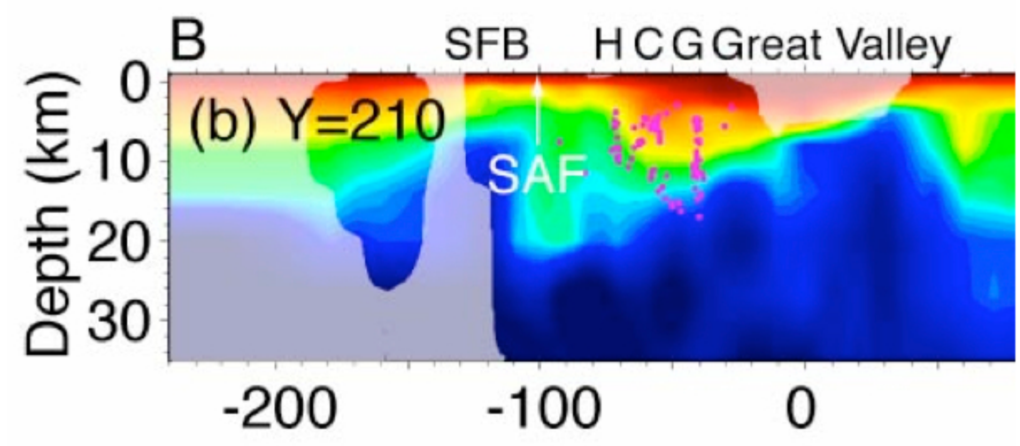

Thurber et al. (2006)

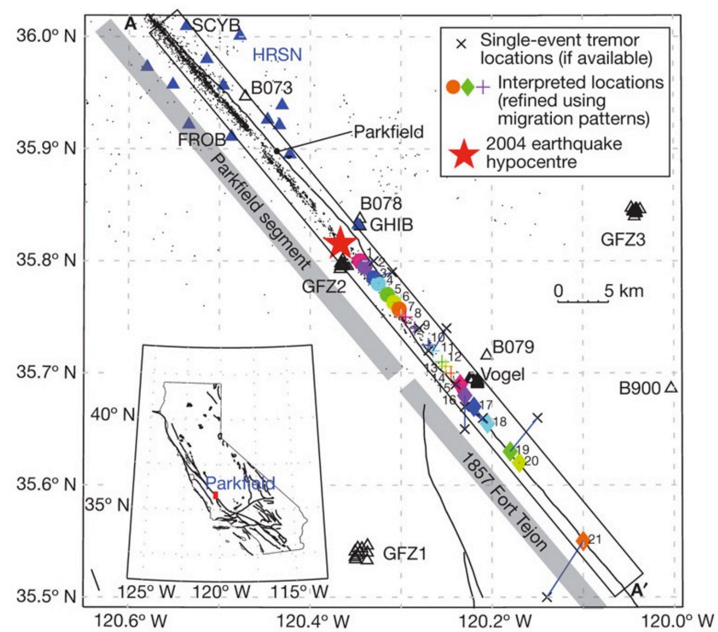

Shelly (2010)

Ductile softening mechanisms

- Thermo-mechanical coupling
- Grain size reduction
- Foliation / fabric development
- Mineral alteration
- Pressure solution
- …

All lead to the development of shear zones and strength reduction

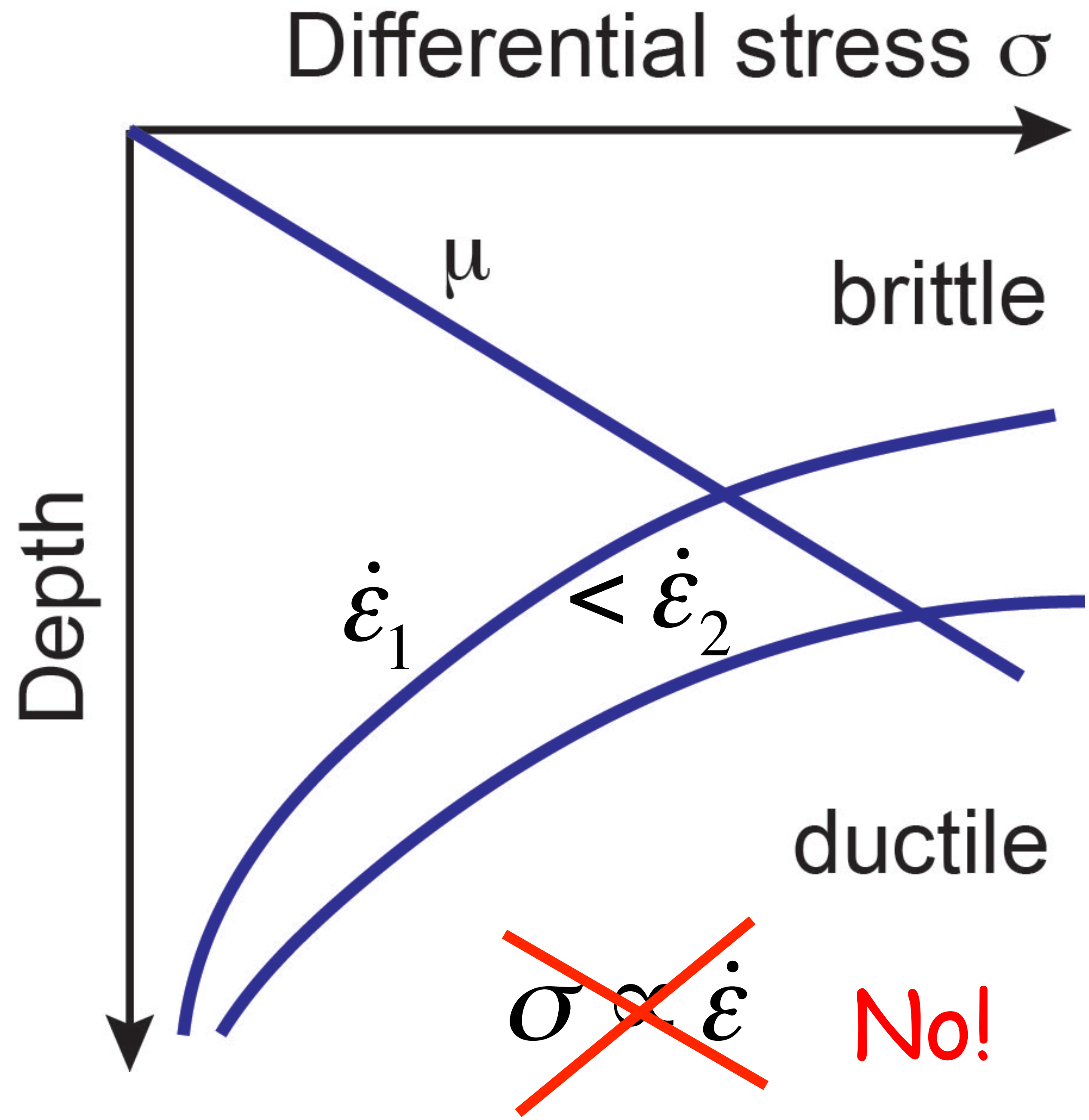
Differential stress σ
Depth
μ
brittle
$\dot{\varepsilon}_1 < \dot{\varepsilon}_2$
ductile
$\sigma \propto \dot{\varepsilon}$
No!

Surface velocity due to a strike-slip fault

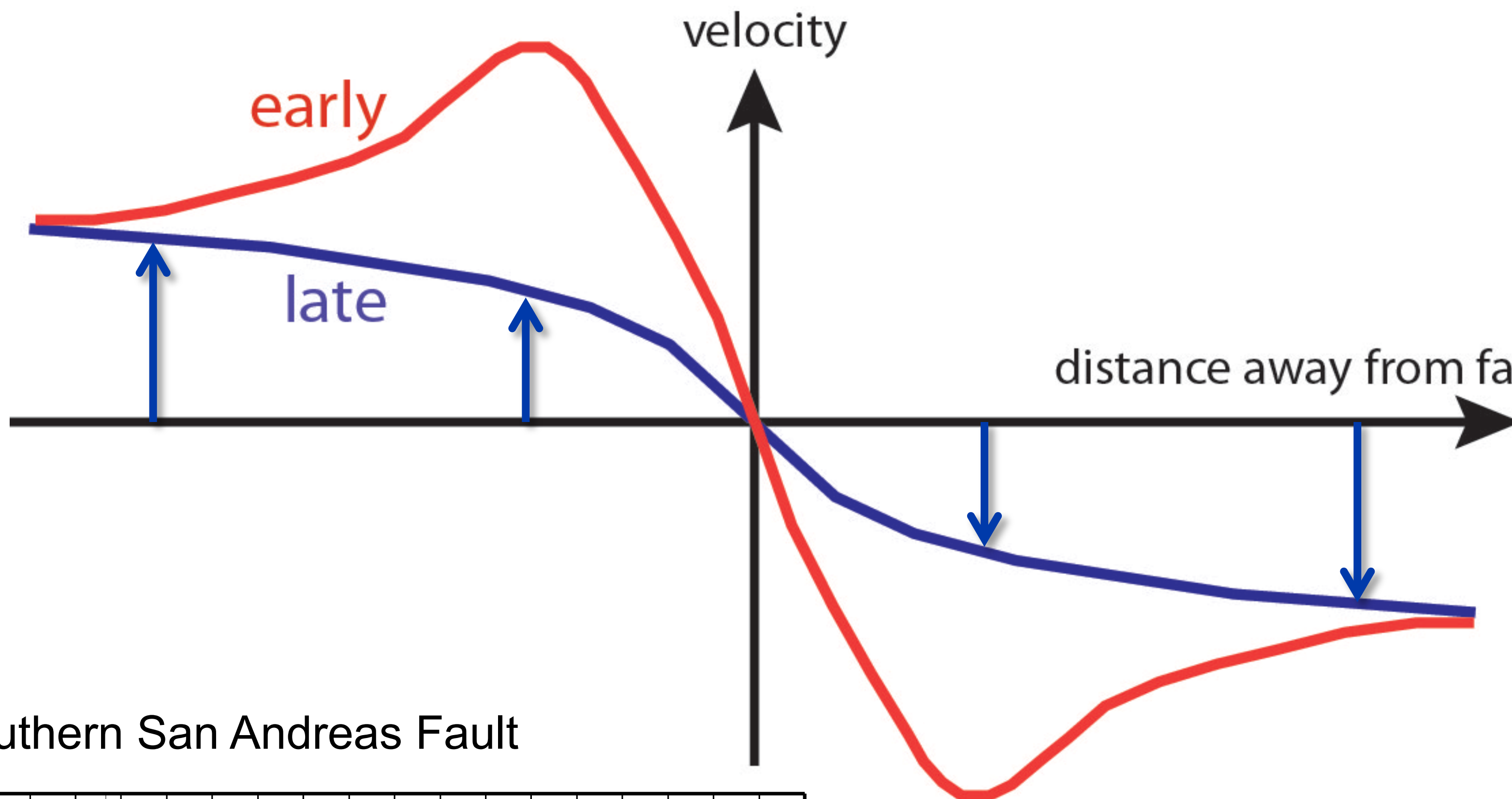

Southern San Andreas Fault

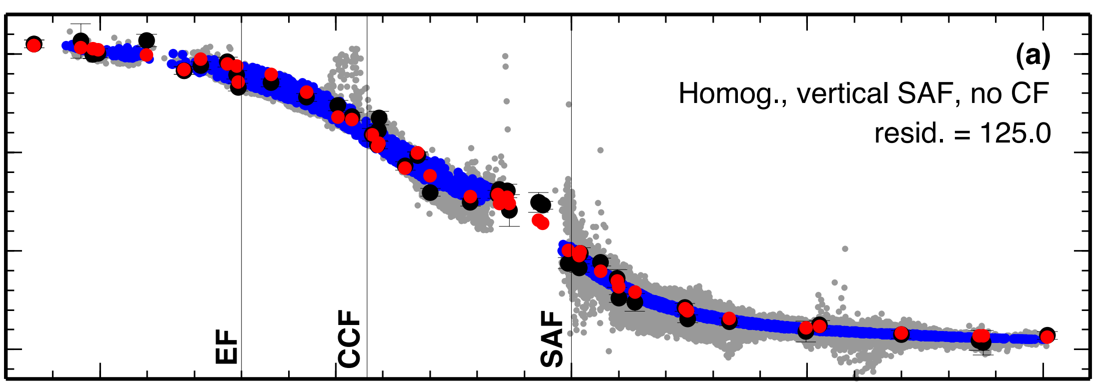

Lindsey & Fialko 2013

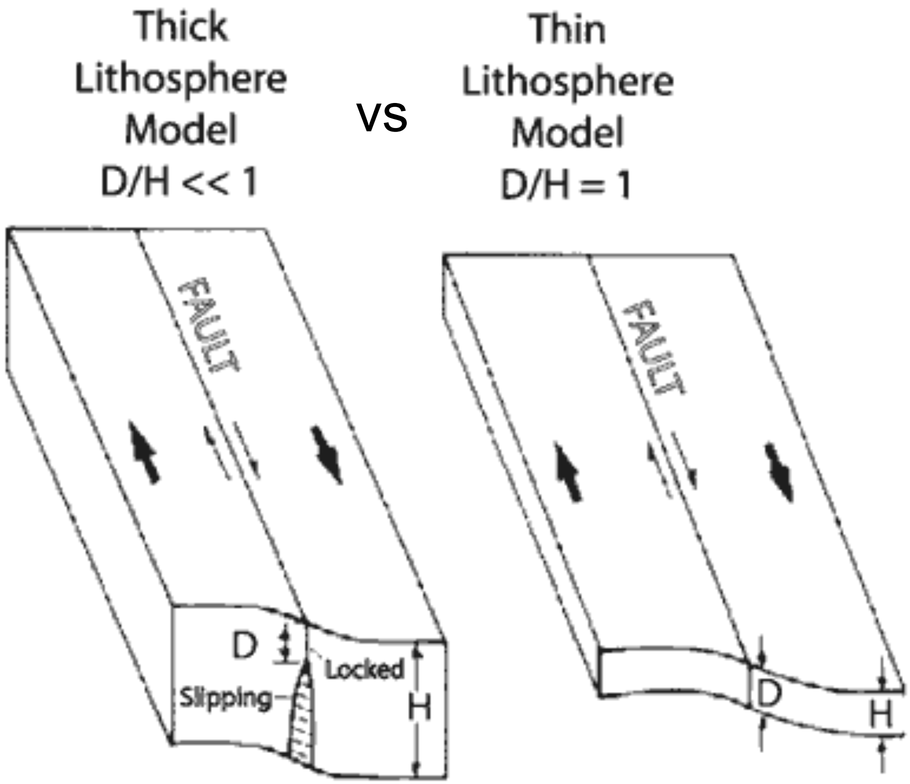

“Fault-block vs Viscous sheet”
“Crème Brûlée vs Jelly Sandwich”
“Bottom-driven vs Side-driven”

Geodetic slip rates and fault locking depths depend on model assumptions

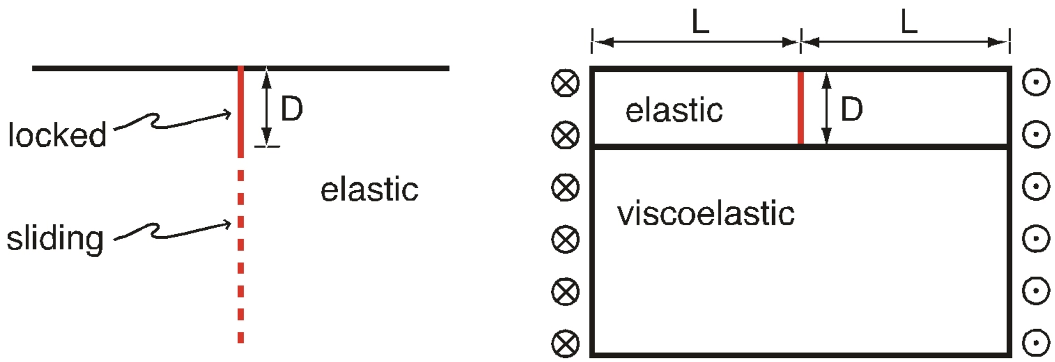

Difference between the models results from oversimplified model assumptions?

Li and Rice, 1987
Johnson and Segall, 2004

Savage and Burford, 1973
Turcotte and Spence, 1974

Elsasser, 1969
Savage and Prescott, 1978

Earthquake cycles on a rate-and-state fault

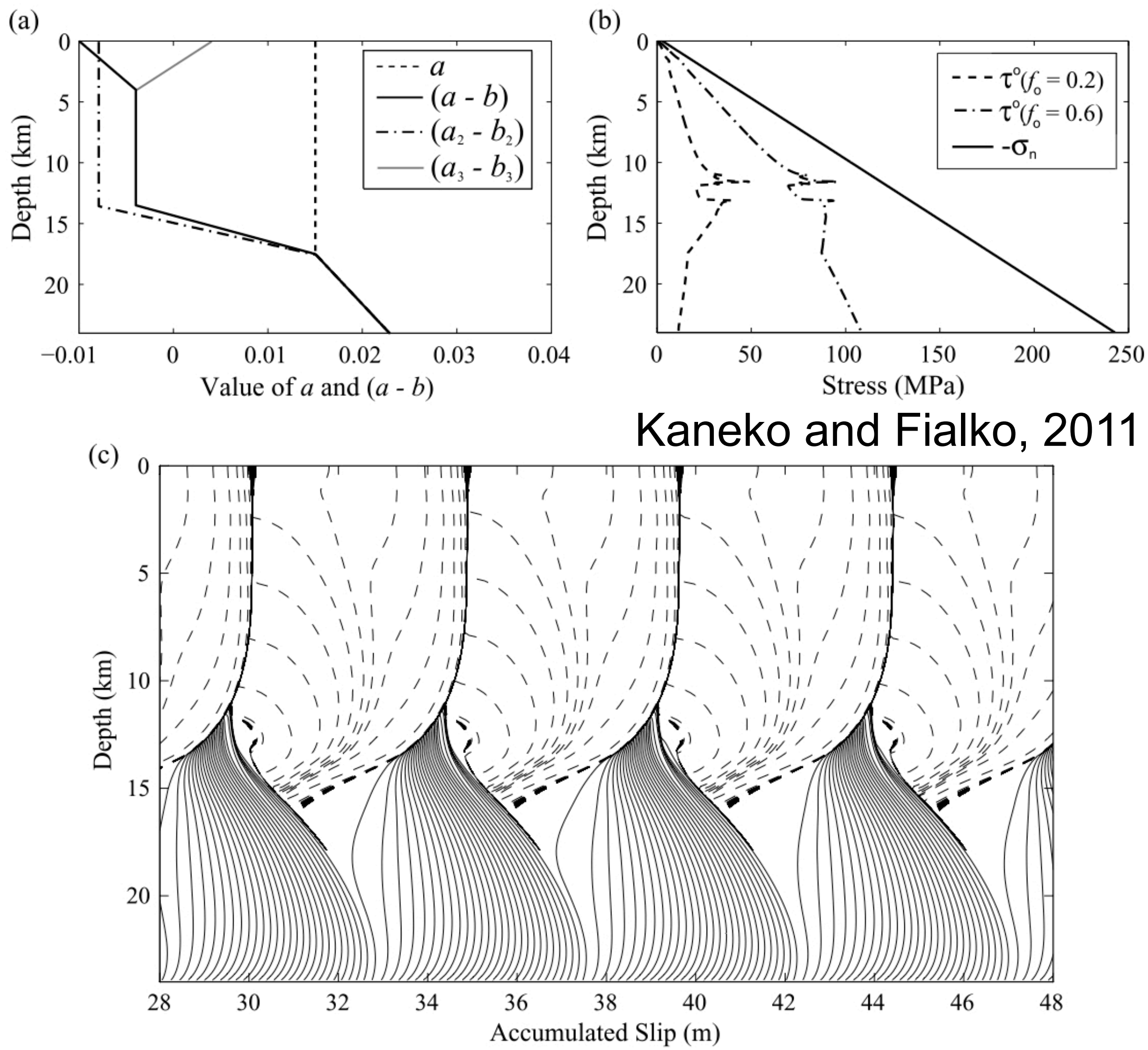

Kaneko and Fialko, 2011

Tse and Rice, 1987

Lapusta et al., 2001

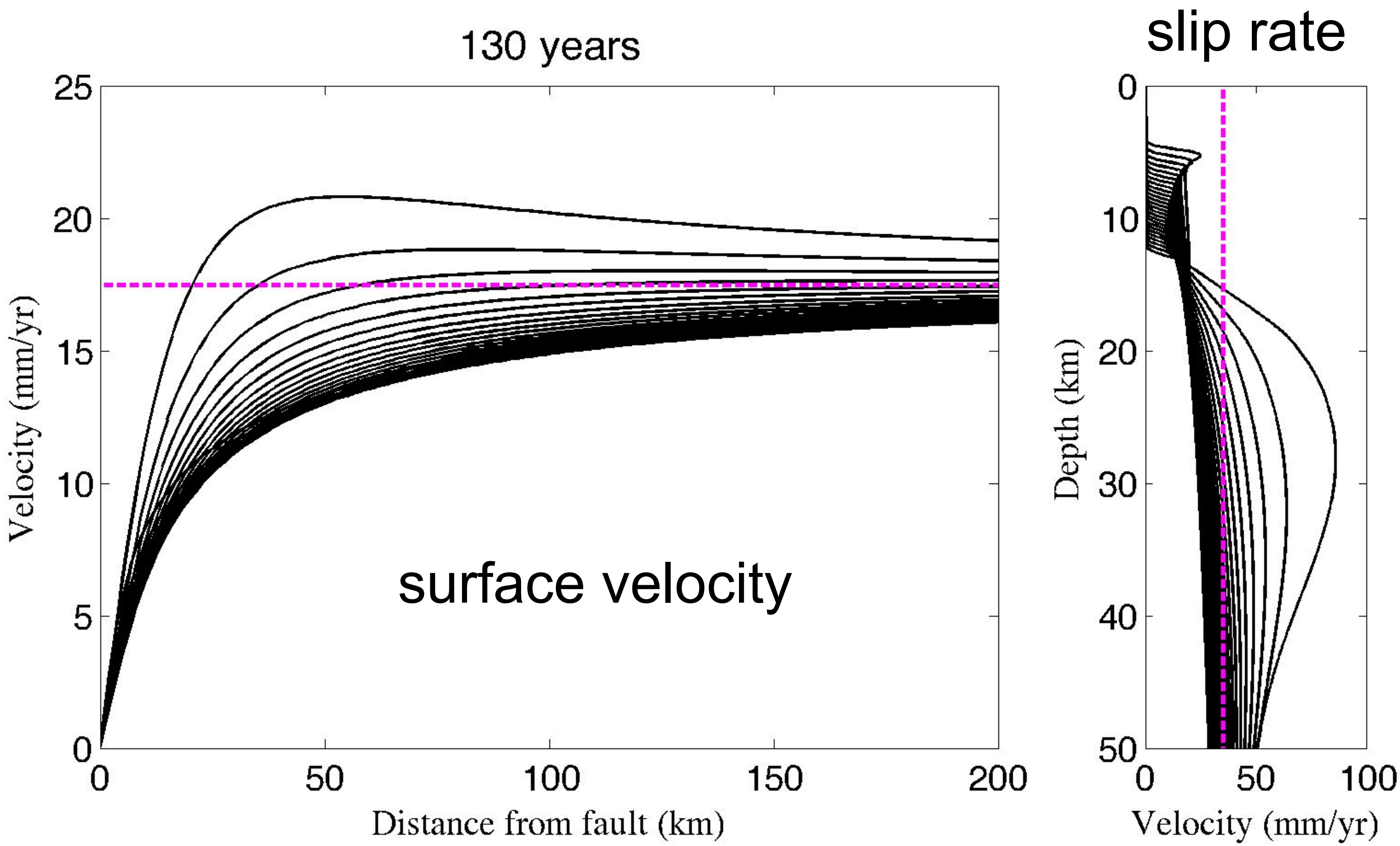
130 years
slip rate
surface velocity
Velocity (mm/yr)
Distance from fault (km)
Depth (km)
Velocity (mm/yr)
25
20
15
10
5
0
0
50
100
150
200
0
10
20
30
40
50
0
50
100

VS

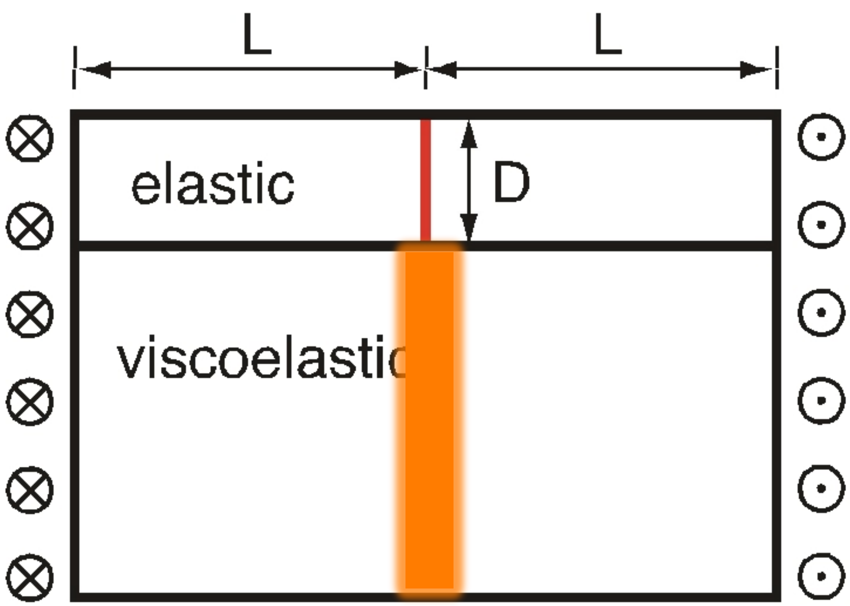

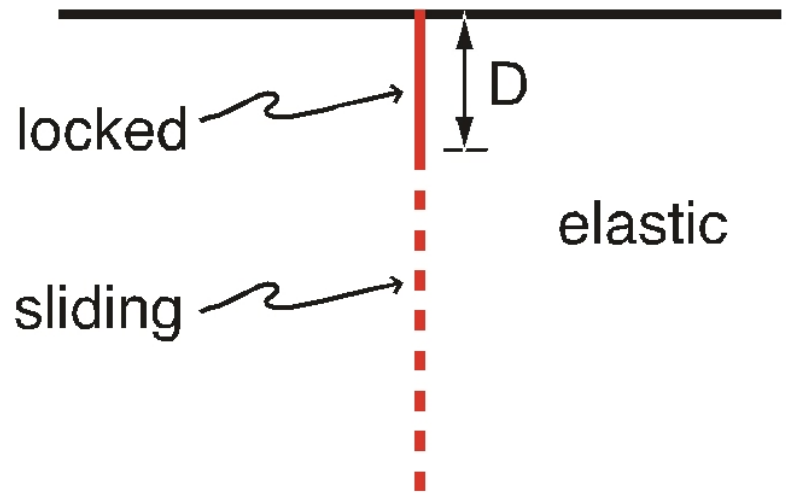

Governing equations

$$\sigma_{ij,j} = 0$$

conservation of momentum

$$\left(kT_{,i}\right)_{,i} + \sigma_{ij}\dot{\varepsilon}_{ij} = c\rho\dot{T}$$

conservation of energy

$$\dot{\varepsilon}_{ij} = F\left(\sigma_{ij}\right)$$

$_{ij}$ constitutive relationship

$$\dot{\varepsilon} = \dot{\varepsilon}_e + \dot{\varepsilon}_v = \frac{1}{2\mu}\dot{\sigma} + \frac{1}{2\eta\left(\sigma,T\right)}\sigma$$

elastic viscous

Effective rheology

$$\dot{\varepsilon}_v = \dot{\varepsilon}_D + \dot{\varepsilon}_G = A_D \sigma^{n_D} + A_G d^{-m} \sigma^{n_G}$$

dislocation creep

diffusion creep

$n_D \sim 3$

$n_G \sim 1$

$m \sim 3$

$r \sim 1$

$$d = d_0 \sigma^{-r}$$

equilibrium grain size

ij

Assuming that the equilibrium grain size is attained when

$$R = \dot{\varepsilon}_D / \dot{\varepsilon}_G \sim O(1)$$

de Bresser et al. (1998; 2001)
Montesi and Hirth (2003)

$$\dot{\varepsilon}_v = \left(1 + 1/R\right) A_D\left(T\right) \sigma^{n_D}$$

Thermo-mechanical coupling in power-law materials with Arrhenius temperature dependence

$$\dot{\varepsilon} = C\sigma^n \exp\left(-\frac{Q}{RT}\right)$$

$$\dot{T} \propto \dot{\varepsilon}\sigma$$

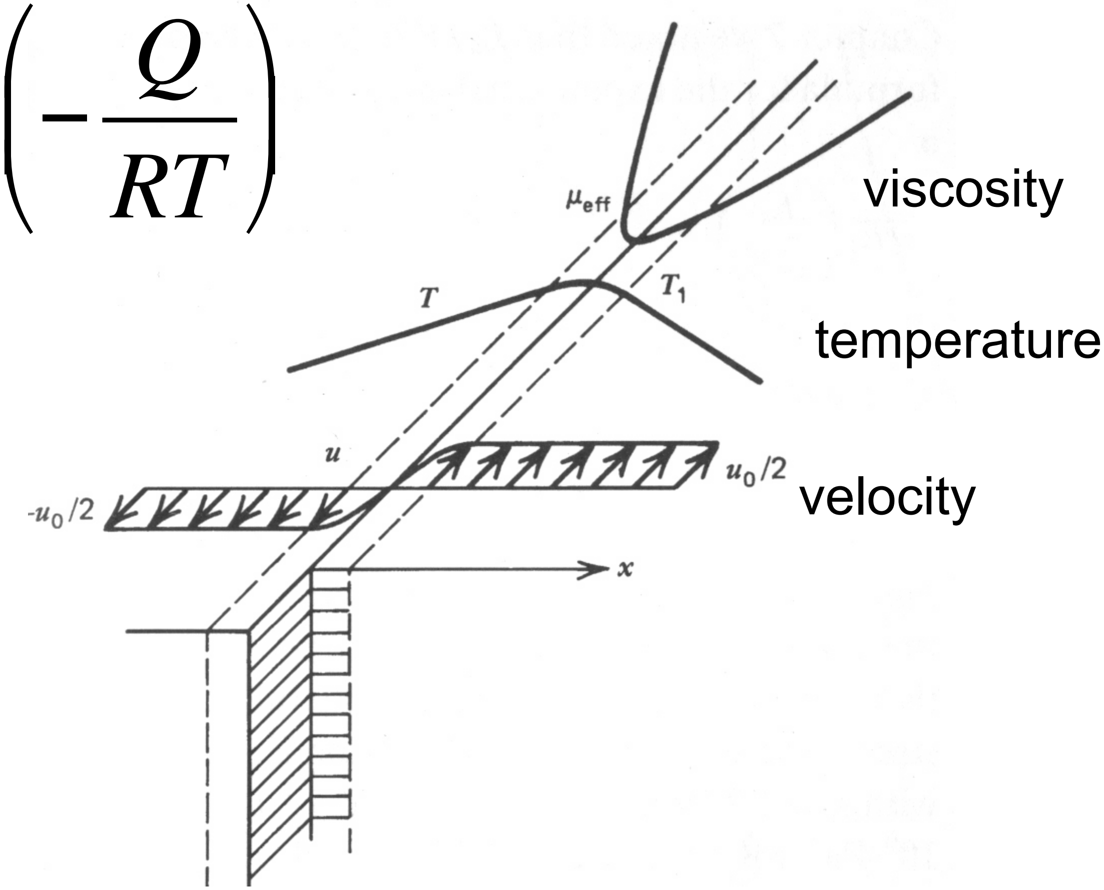

Yuen et al., 1978; Fleitout and Frodivaux, 1980; Turcotte and Schubert, 2002

Thermo-mechanical coupling in power-law materials with Arrhenius temperature dependence

$$k\frac{\partial^2 T}{\partial x^2} \sim \dot{\varepsilon}\sigma$$

$$\dot{\varepsilon} = A\sigma^n$$

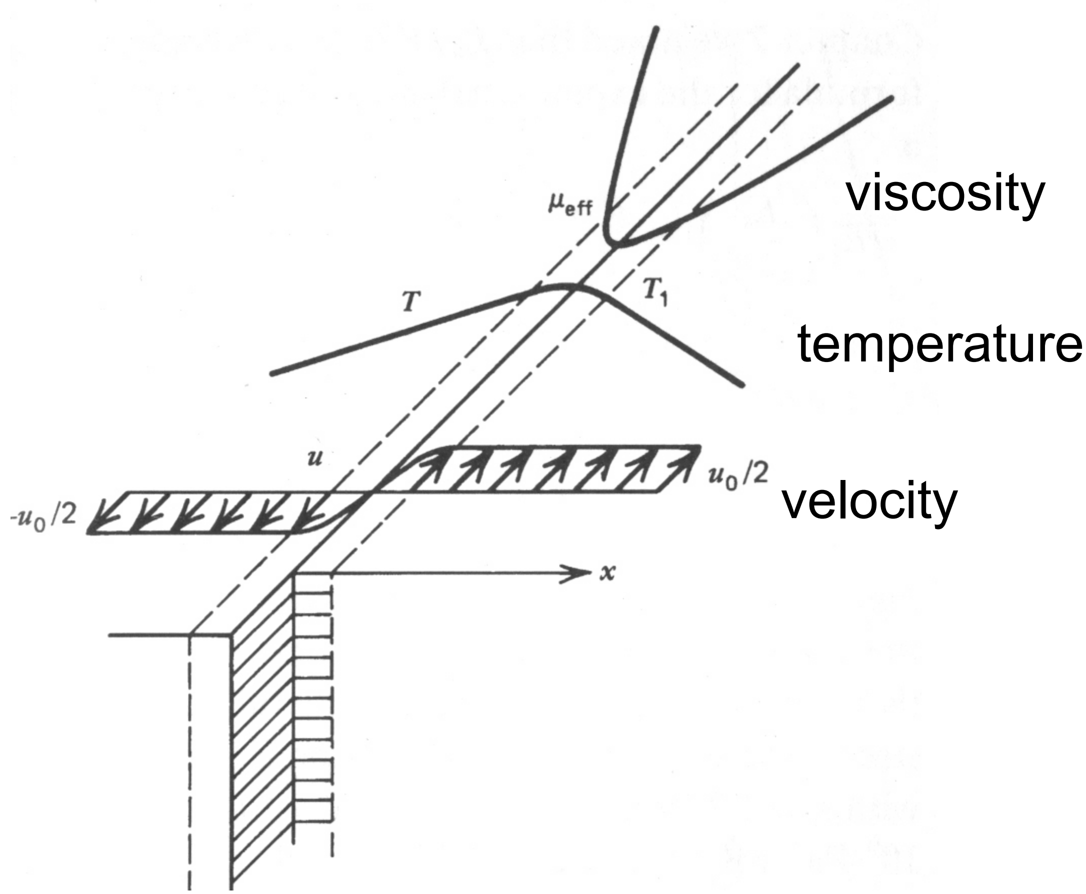

Yuen et al., 1978; Fleitout and Frodivaux, 1980; Turcotte and Schubert, 2002

Thermo-mechanical coupling in power-law materials with Arrhenius temperature dependence

$$k\frac{\Delta T}{D^2} \sim A^{-1/n}\dot{\varepsilon}^{(1+1/n)}$$

$$\dot{\varepsilon} \propto \frac{u_0}{D}$$

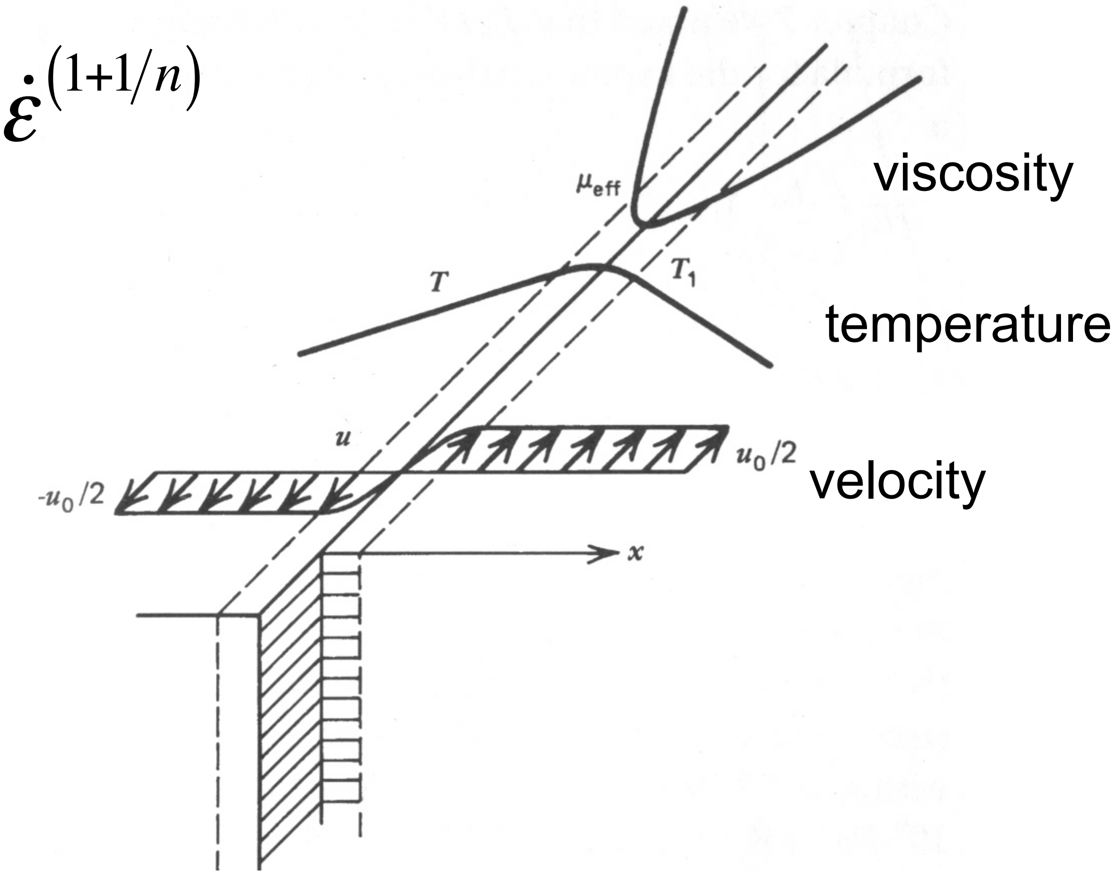

D width of the shear zone

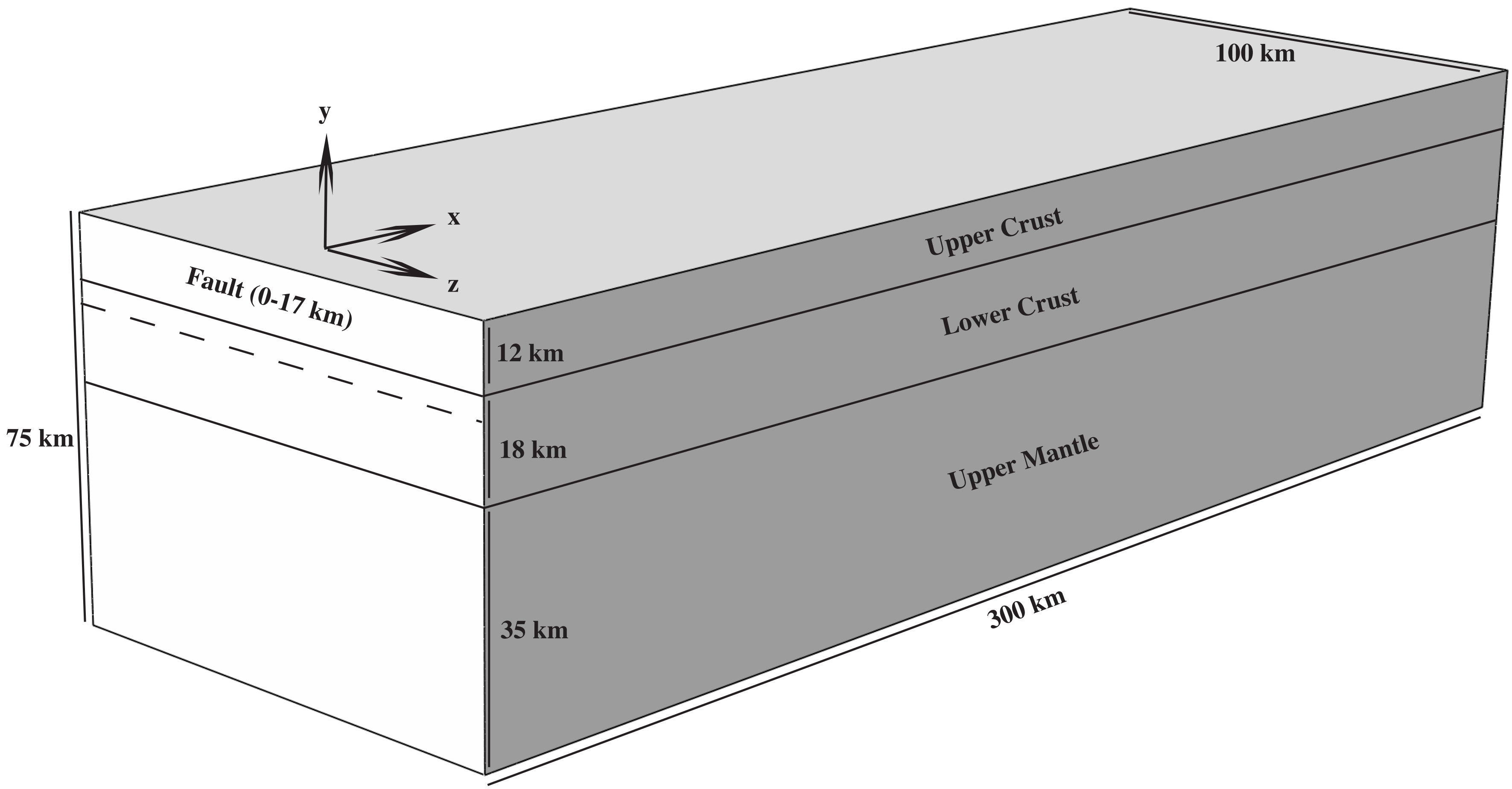

Takeuchi and Fialko, 2012

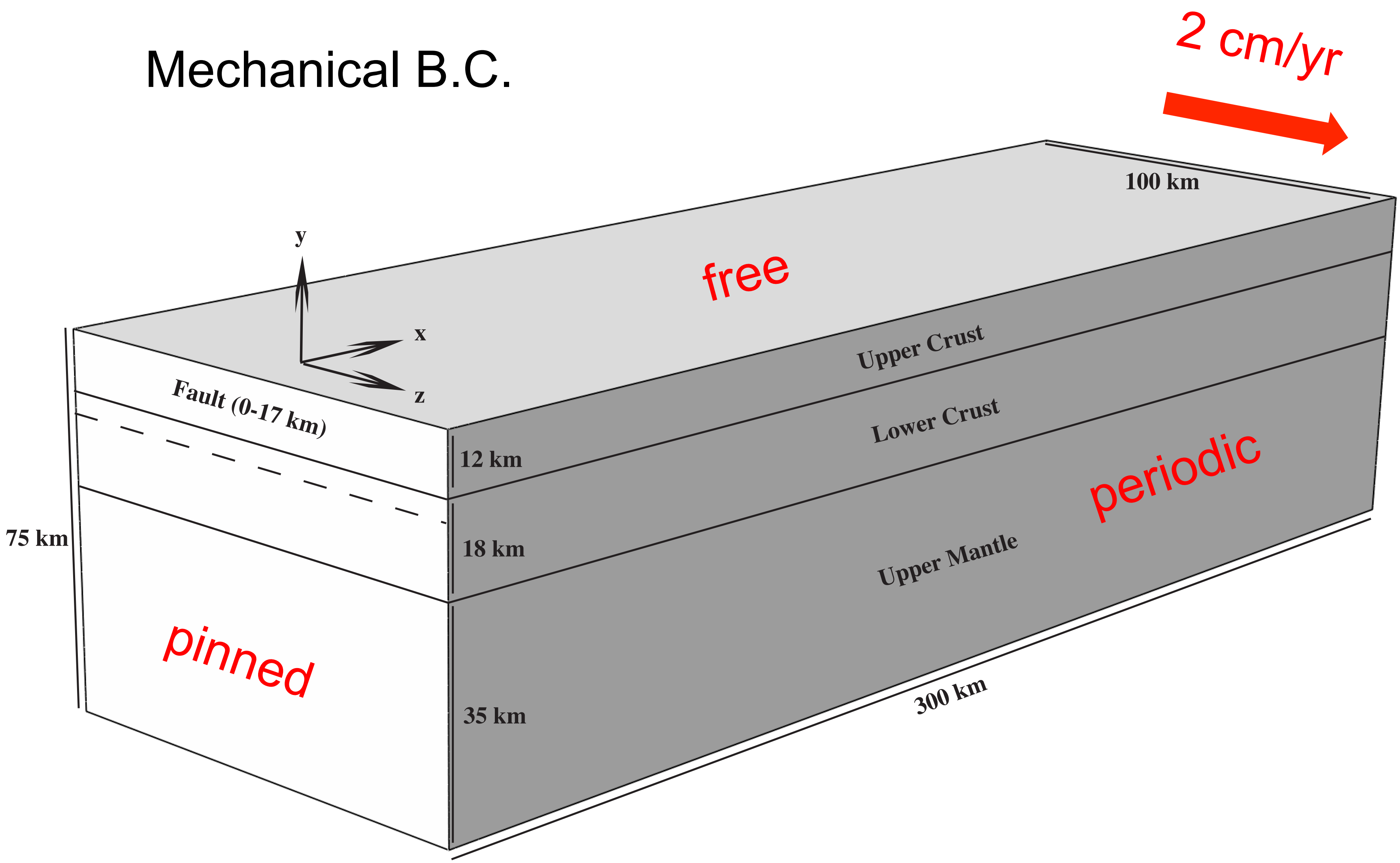

Mechanical B.C.
2 cm/yr
100 km
y
x
z
free
Upper Crust
Lower Crust
Fault (0-17 km)
12 km
18 km
35 km
75 km
periodic
Upper Mantle
pinned
300 km

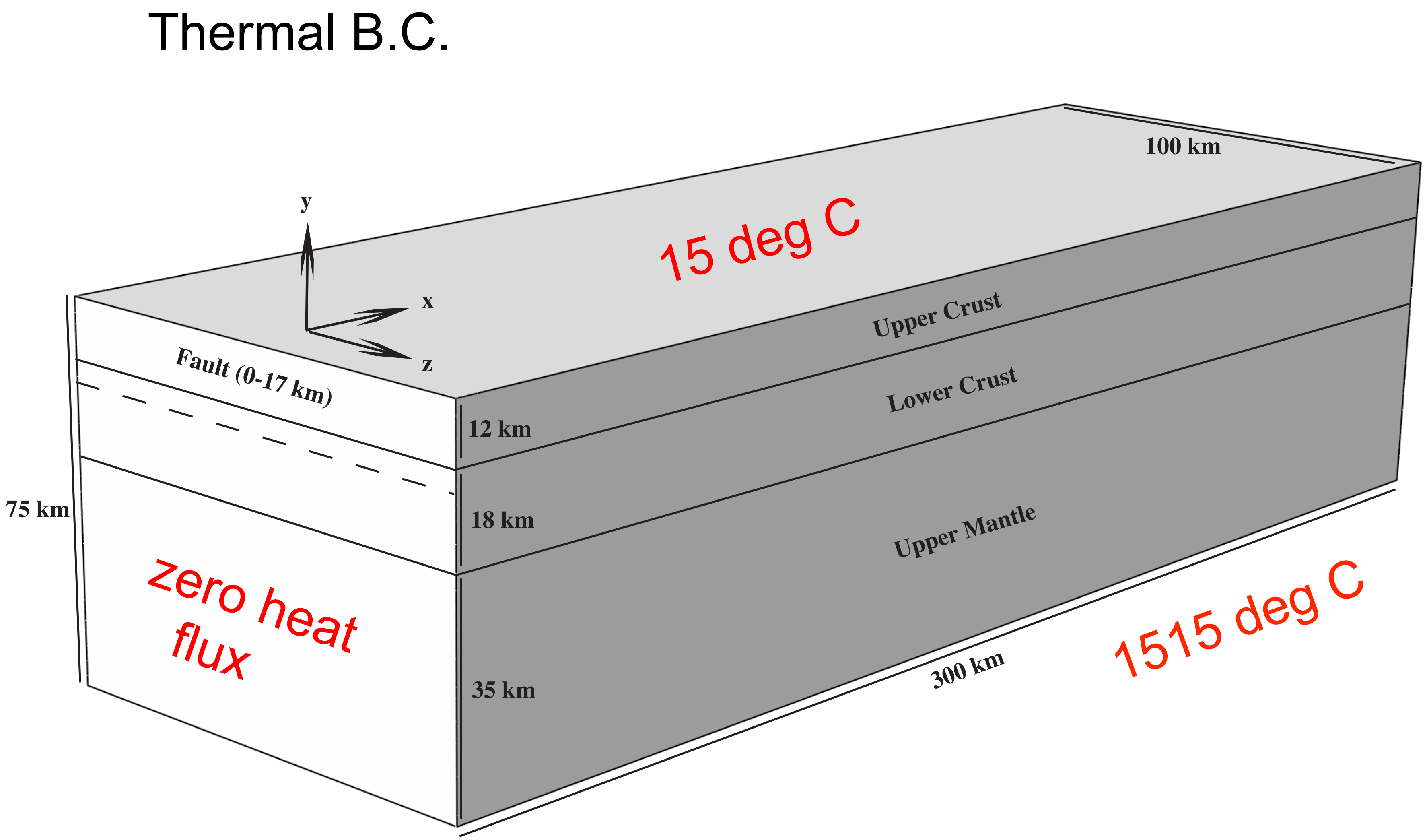

Thermal B.C.
100 km
y
x
z
15 deg C
Upper Crust
Fault (0-17 km)
Lower Crust
12 km
75 km
18 km
Upper Mantle
zero heat flux
1515 deg C
300 km
35 km

Model "spin-up": 20 Ma of steady slip followed by eq cycles

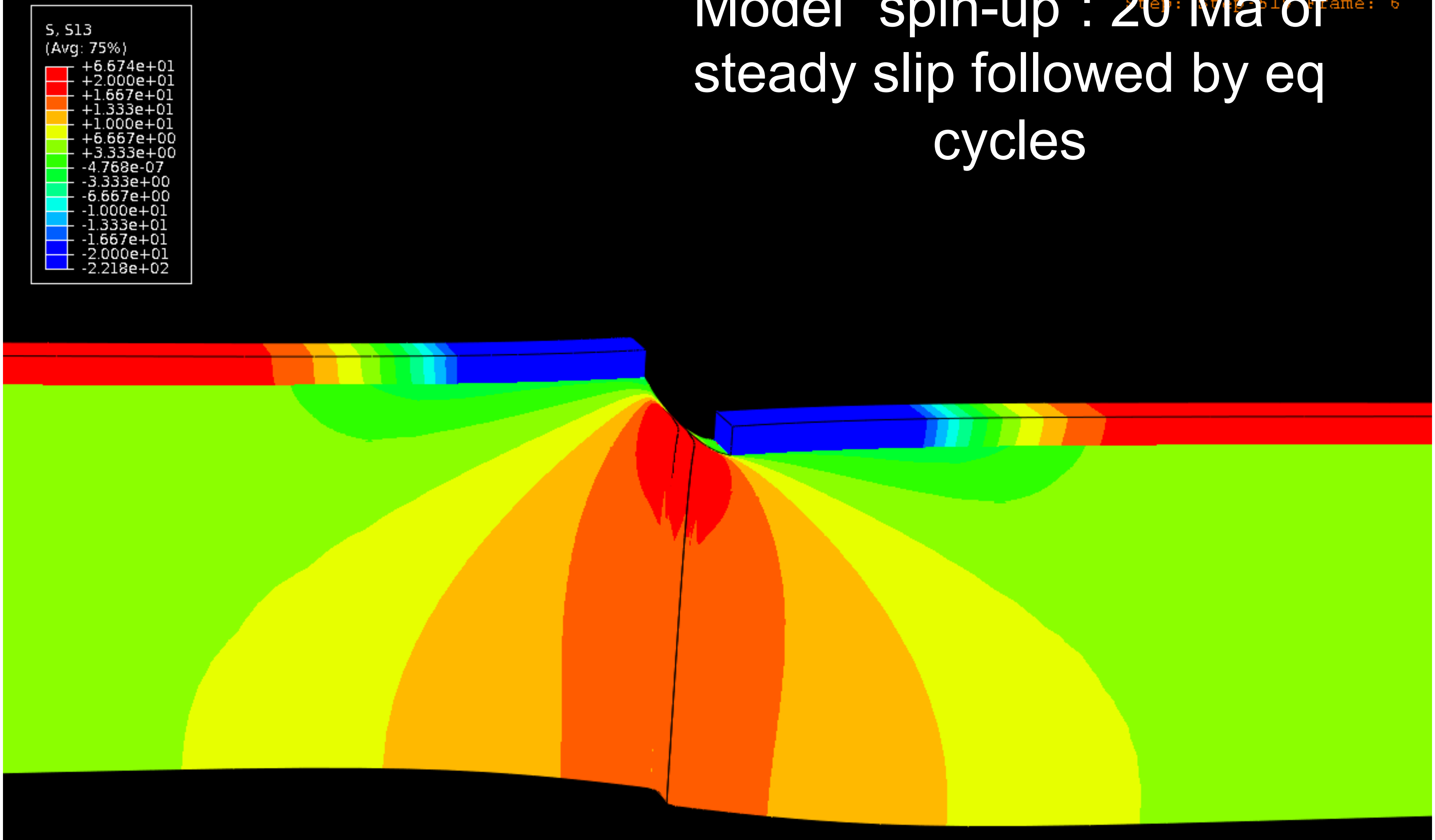

stress

Rheologic end-members: The Matrix

Linear Maxwell T_r = 2000 yrs (M2000)	Power-law Dry gabbro/ olivine Non-coupled Kinematic (DNK)	Power-law Dry gabbro/ olivine Coupled Kinematic (DCK)	Power-law Dry gabbro/ olivine Coupled Stress-controlled (DCS)
Linear Maxwell T_r = 20 yrs (M20)	Power-law Wet gabbro/ olivine Non-coupled Kinematic (WNK)	Power-law Wet gabbro/ olivine Coupled Kinematic (WCK)	Power-law Wet gabbro/ olivine Coupled Stress-controlled (WCS)

Shear stress

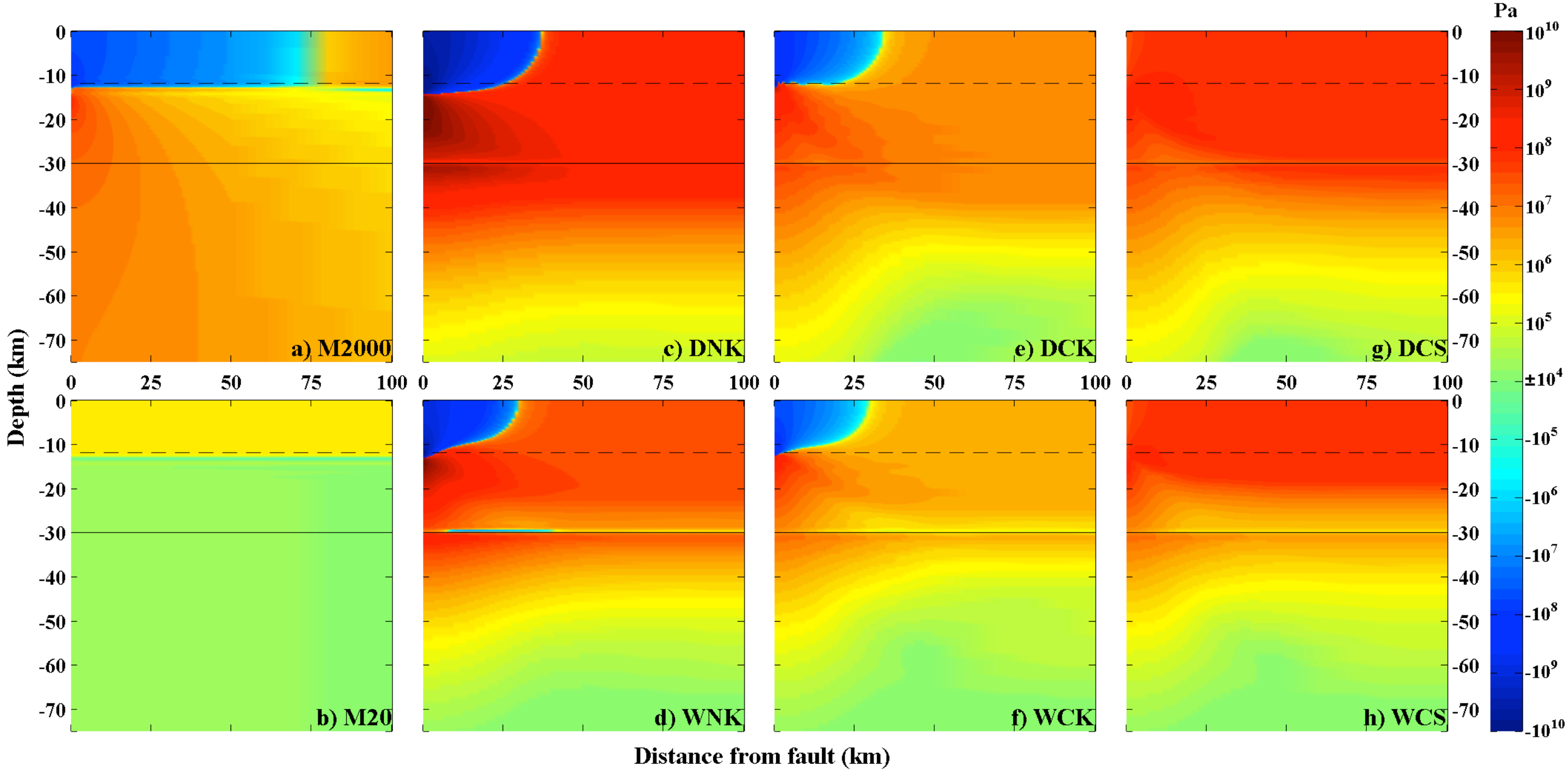

Takeuchi and Fialko, 2012

Model “spin-up”: toward cycle-invariant stress

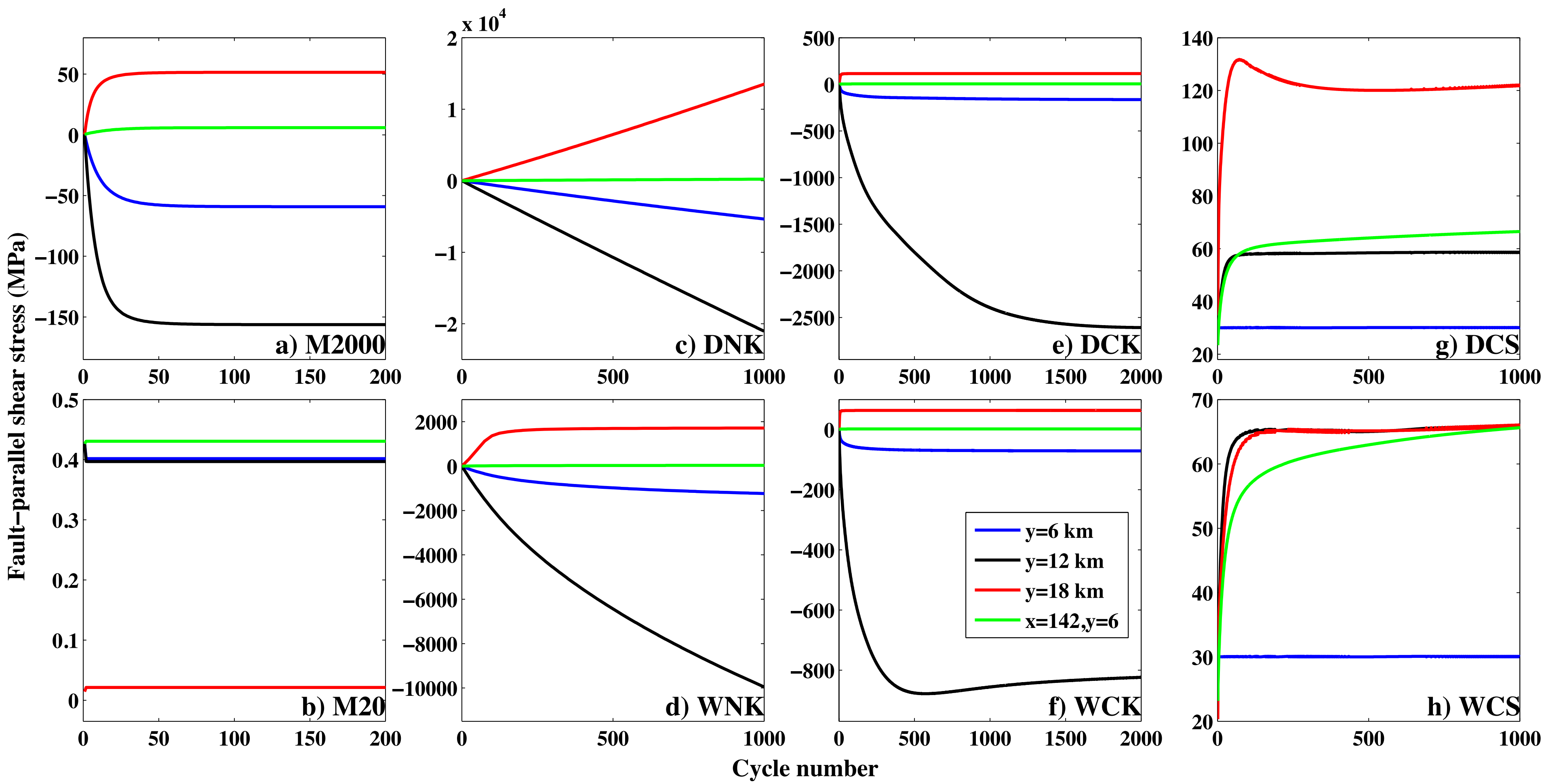

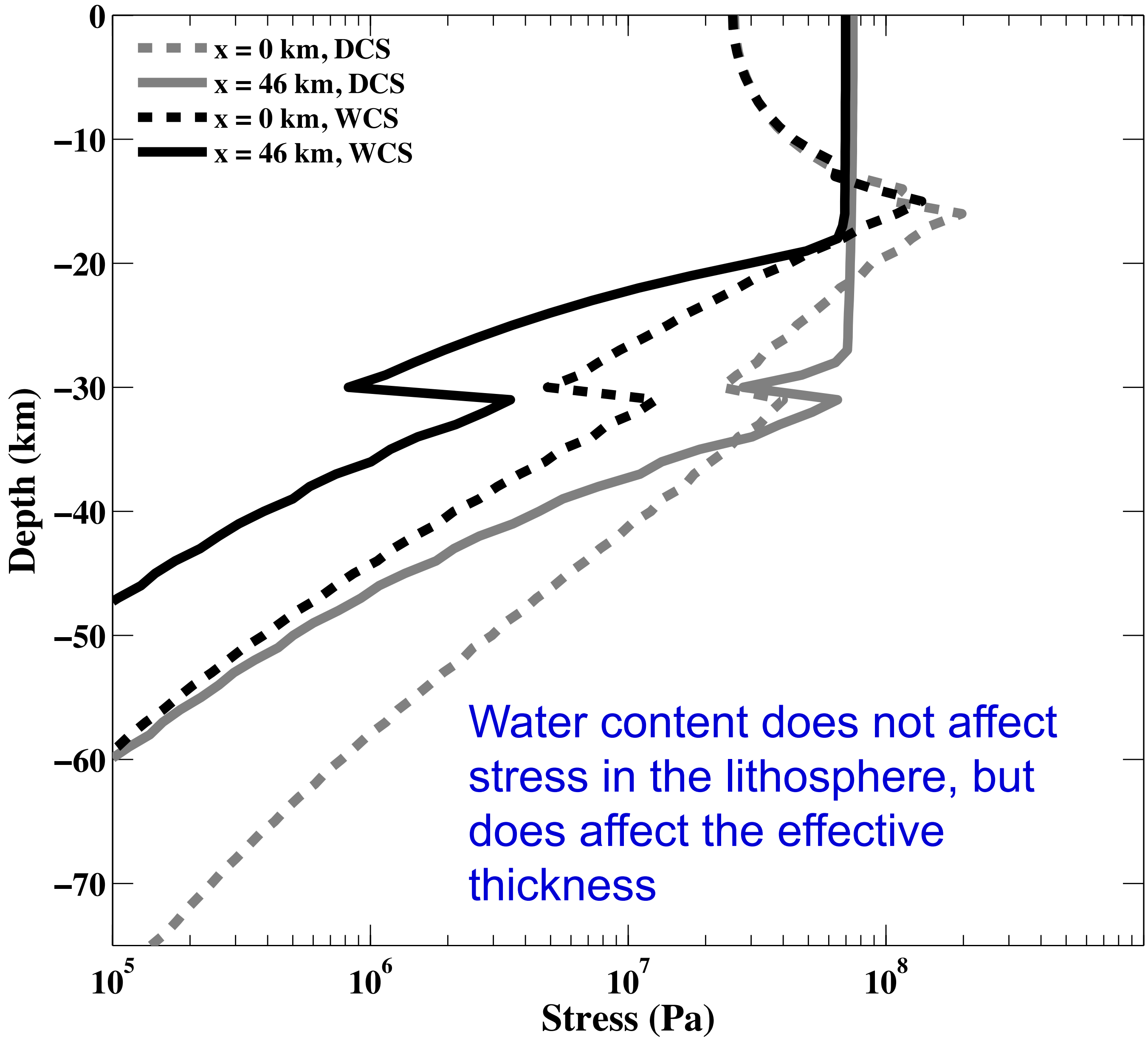

Water content does not affect stress in the lithosphere, but does affect the effective thickness

Constraints from the rock record

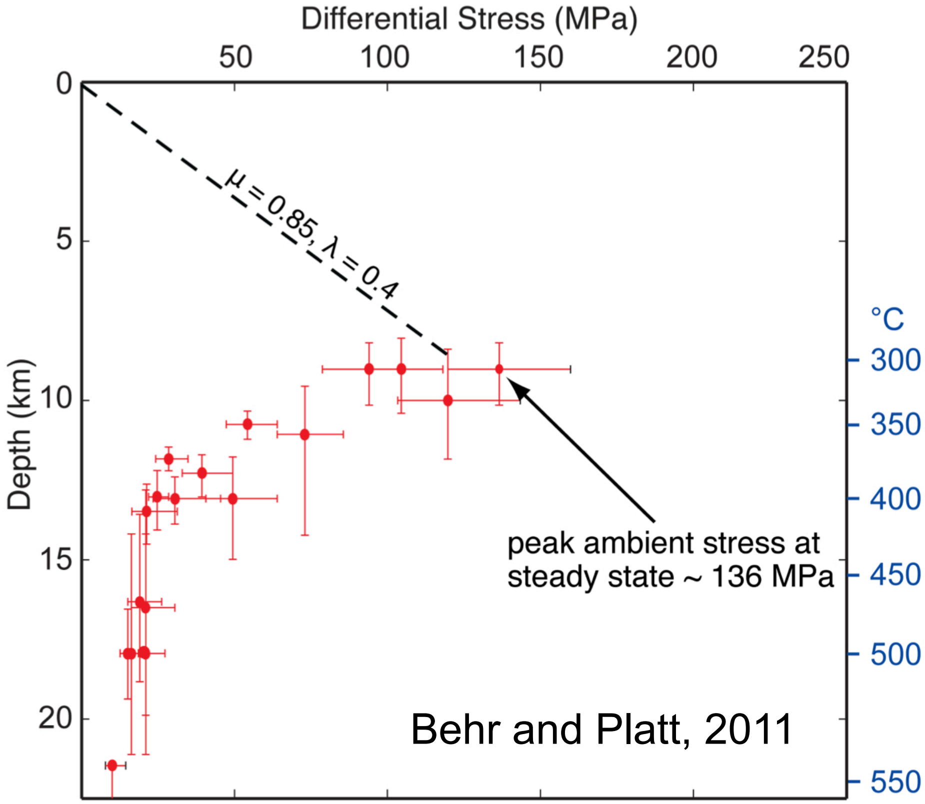

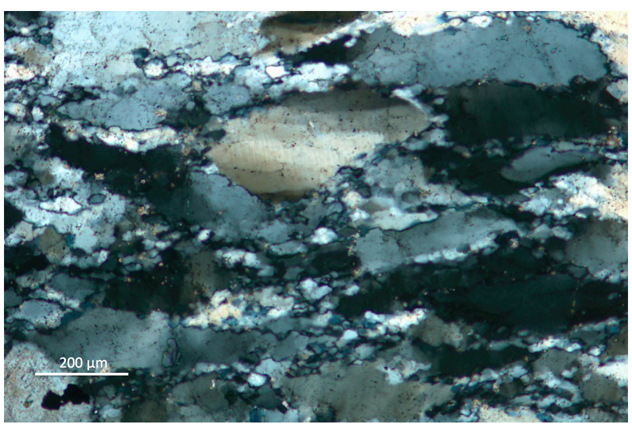

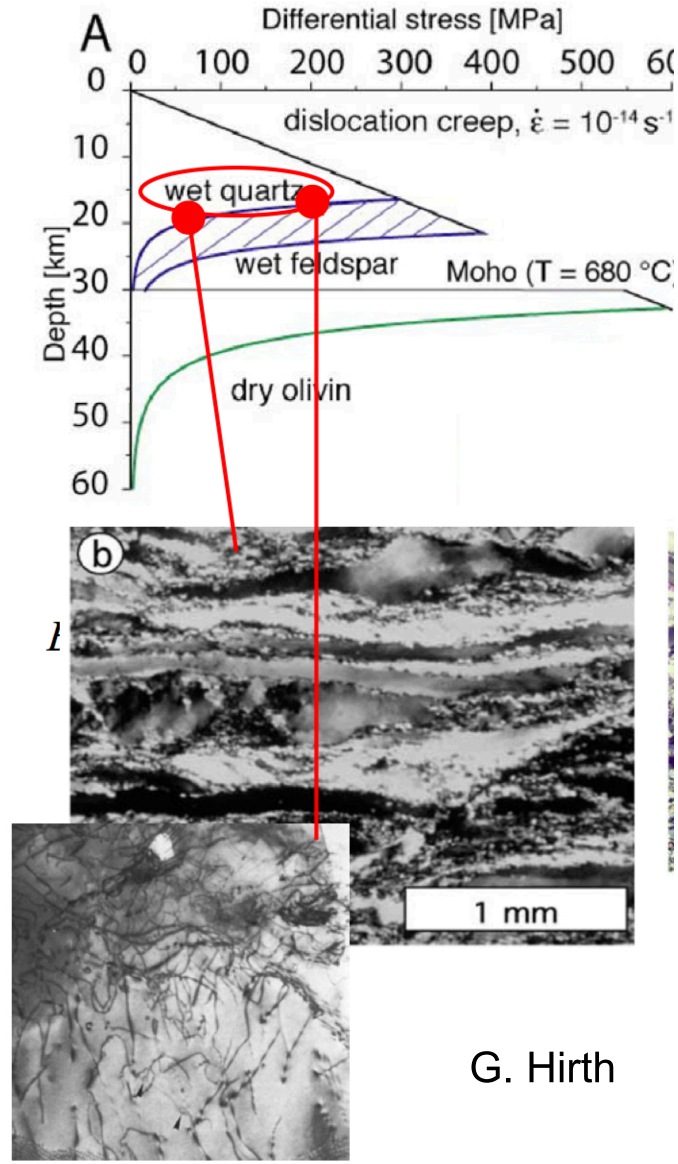

G. Hirth

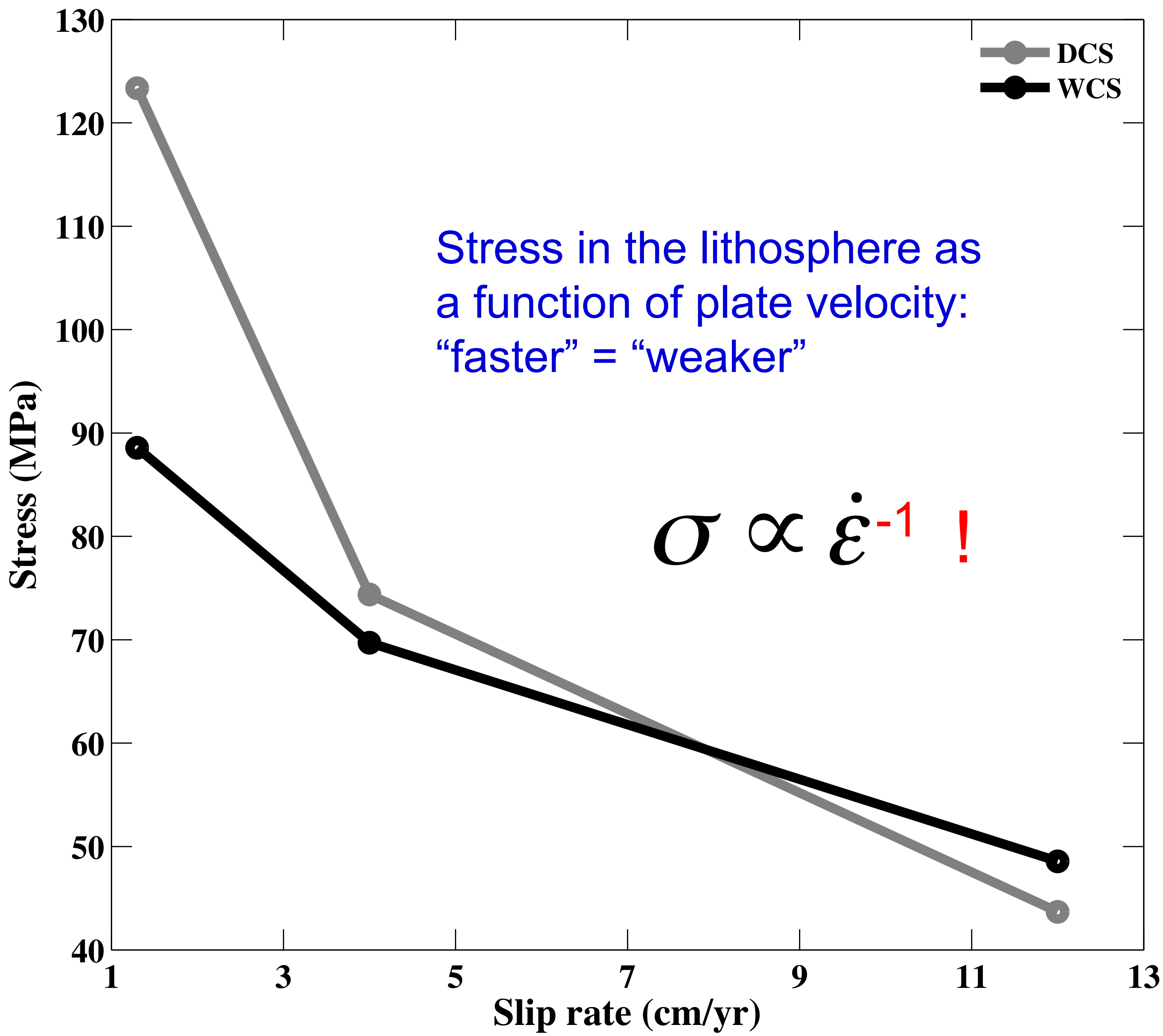

DCS
WCS
Stress in the lithosphere as
a function of plate velocity:
“faster” = “weaker”
$\sigma \propto \dot{\varepsilon}^{-1}$!
Stress (MPa)
Slip rate (cm/yr)
130
120
110
100
90
80
70
60
50
40
1
3
5
7
9
11
13

Strain rate

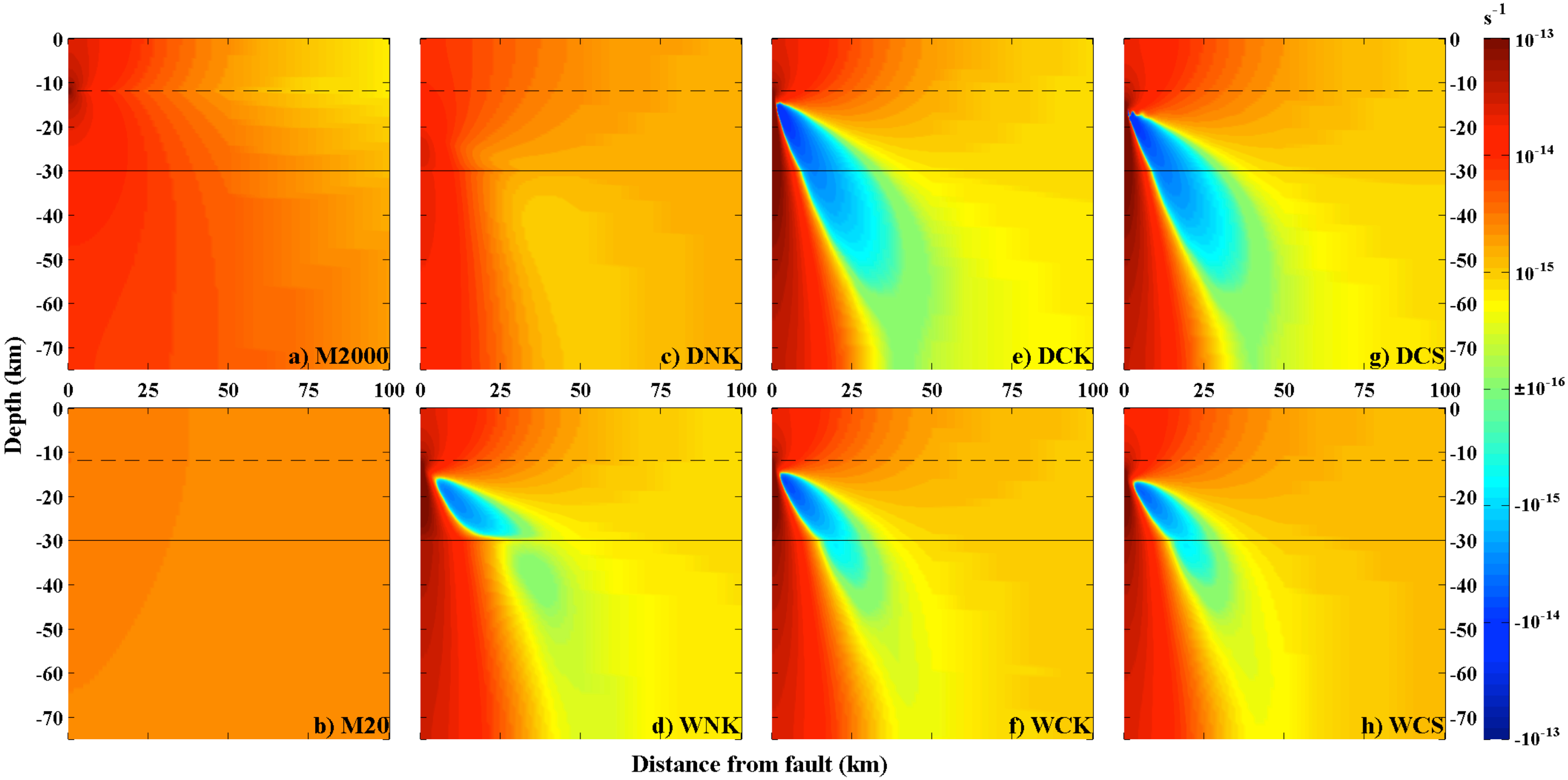

a) M2000
b) M20
c) DNK
d) WNK
e) DCK
f) WCK
g) DCS
h) WCS
Depth (km)
Distance from fault (km)
s-1
10-13
10-14
10-15
±10-16
-10-15
-10-14
-10-13

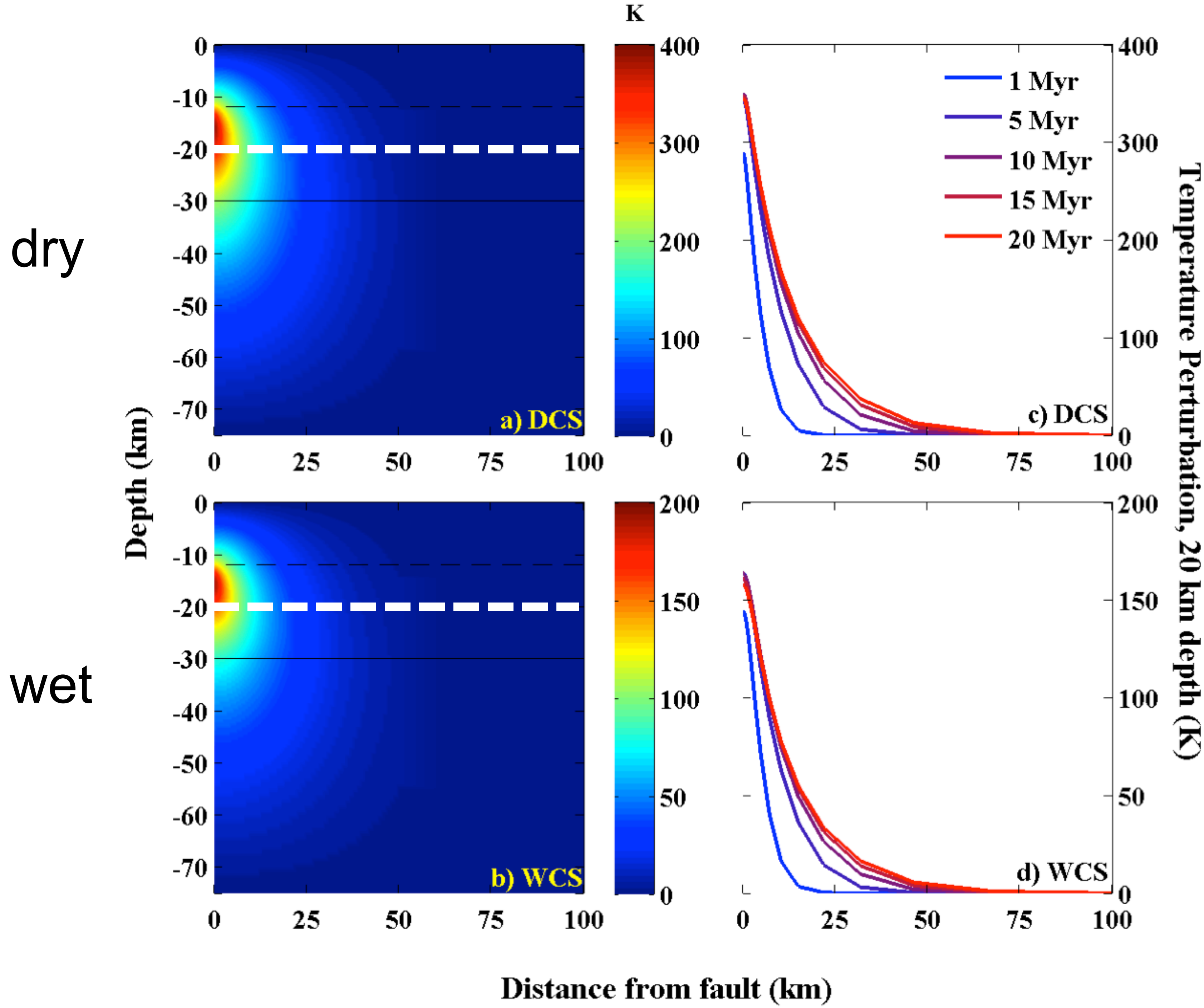

dry
wet
K
a) DCS
b) WCS
c) DCS
d) WCS
1 Myr
5 Myr
10 Myr
15 Myr
20 Myr
Depth (km)
Distance from fault (km)
Temperature Perturbation, 20 km depth (K)

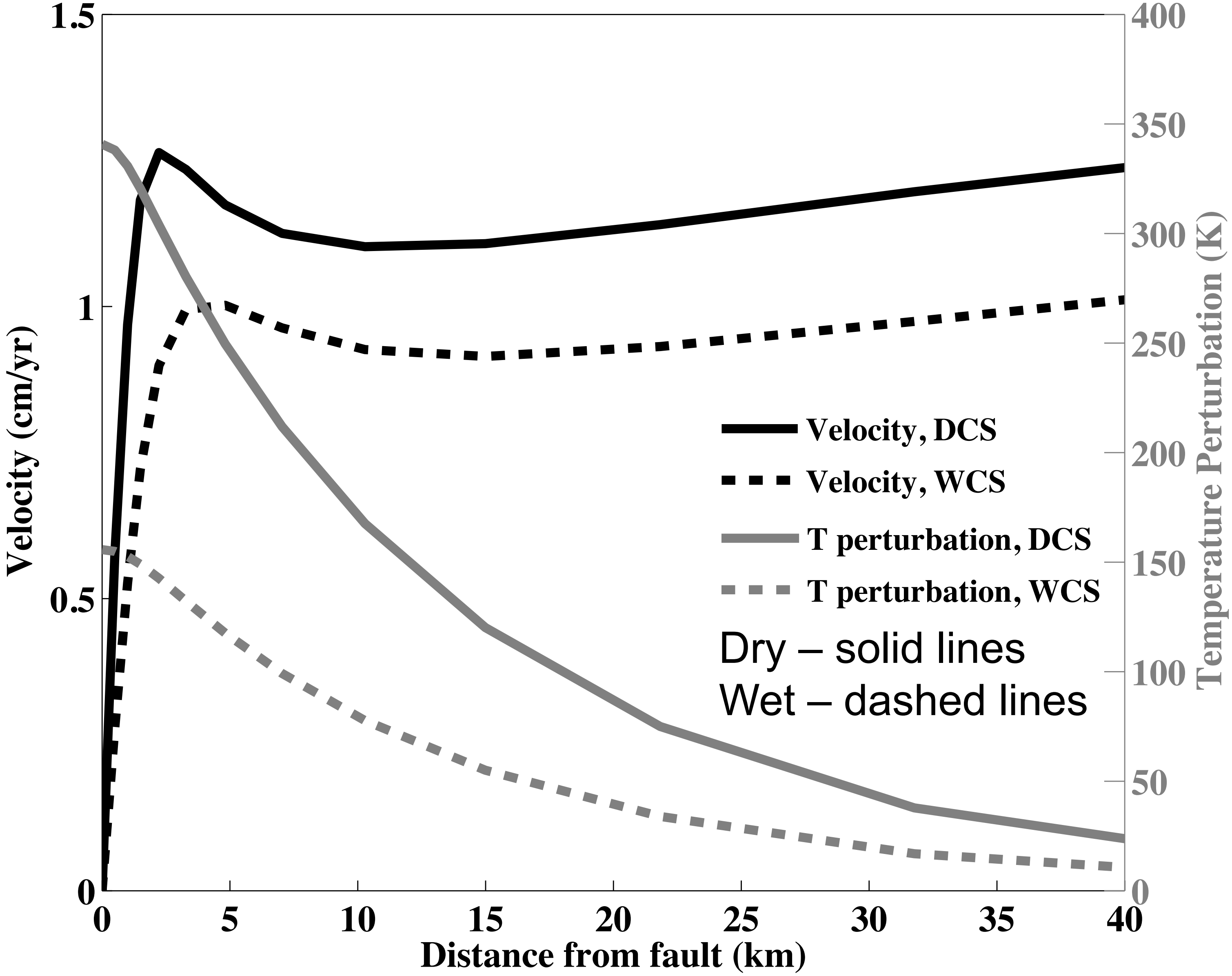

1.5
1
0.5
0
Velocity (cm/yr)
400
350
300
250
200
150
100
50
0
Temperature Perturbation (K)
0
5
10
15
20
25
30
35
40
Distance from fault (km)
Velocity, DCS
Velocity, WCS
T perturbation, DCS
T perturbation, WCS
Dry – solid lines
Wet – dashed lines

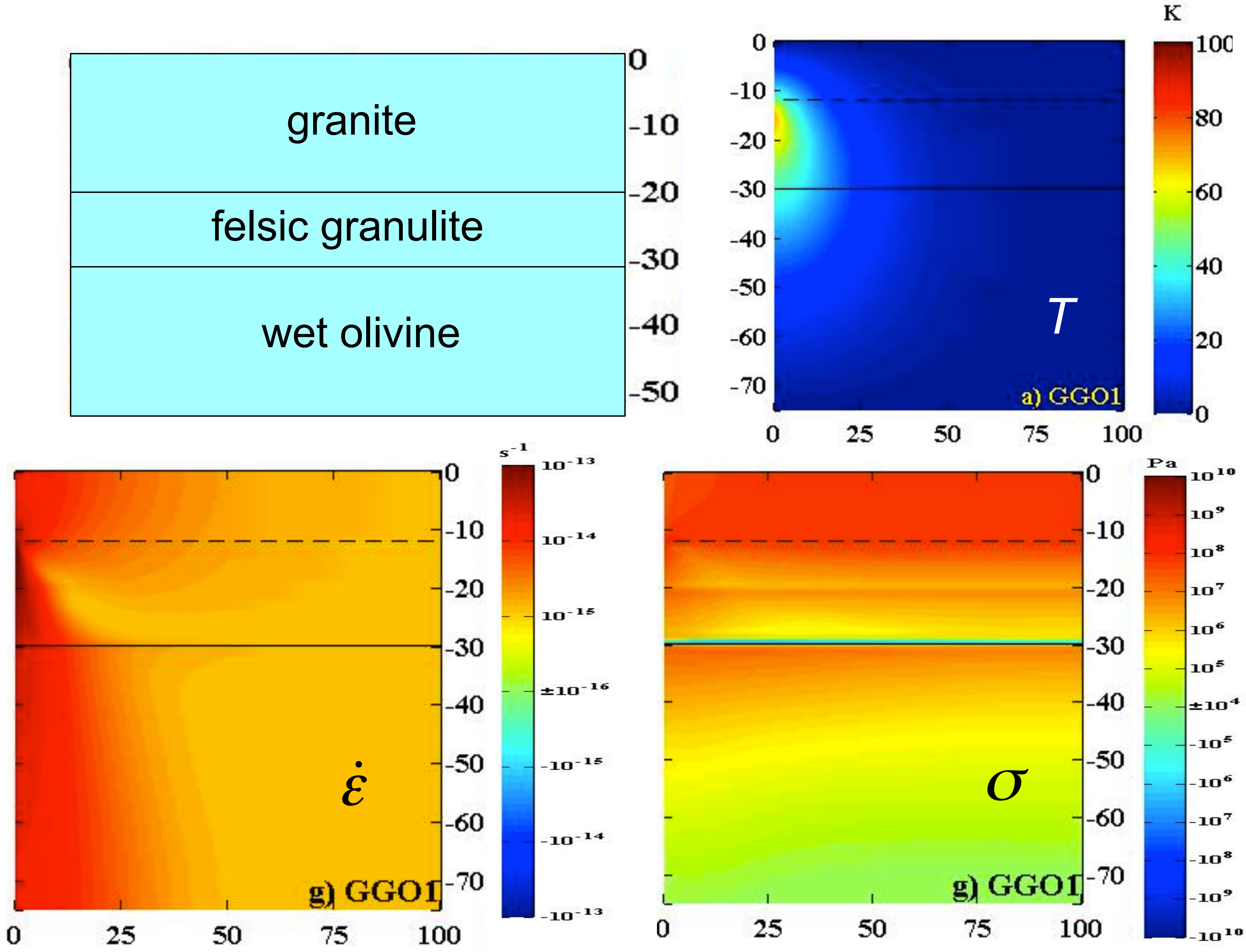

granite
felsic granulite
wet olivine
0
-10
-20
-30
-40
-50
K
T
a) GGO1
0 25 50 75 100
$\dot{\varepsilon}$
s^{-1}
g) GGO1
σ
Pa
g) GGO1

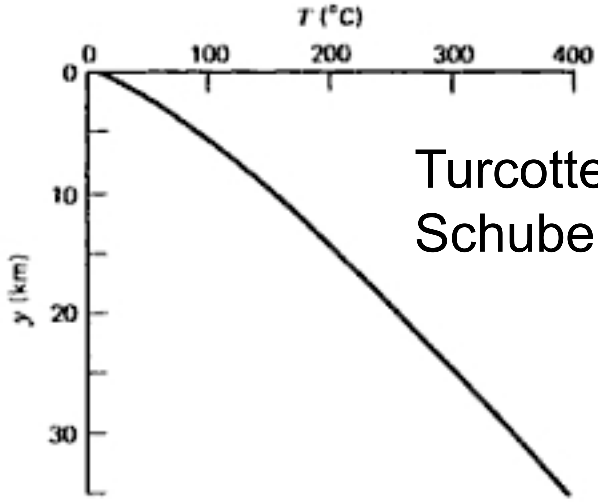

4–12 A typical geotherm in the continental crust.

Turcotte and Schubert (2002)

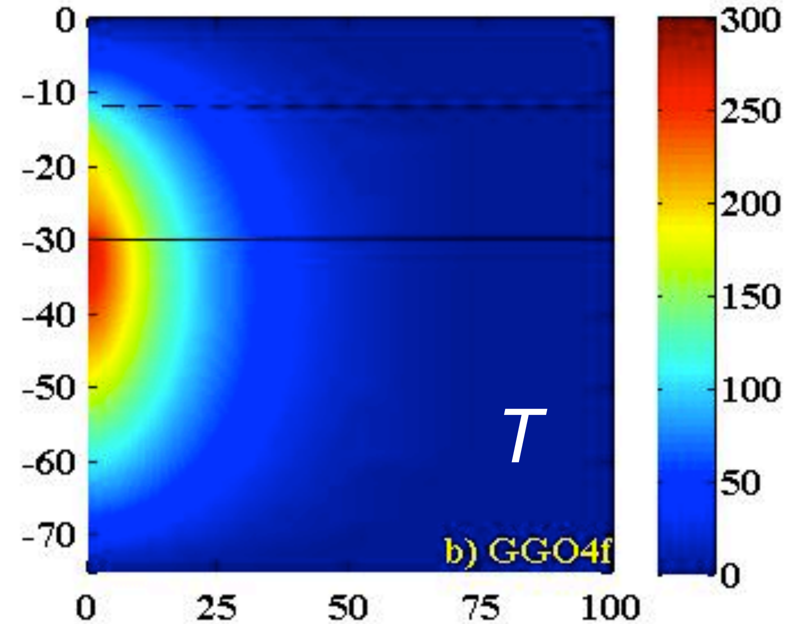

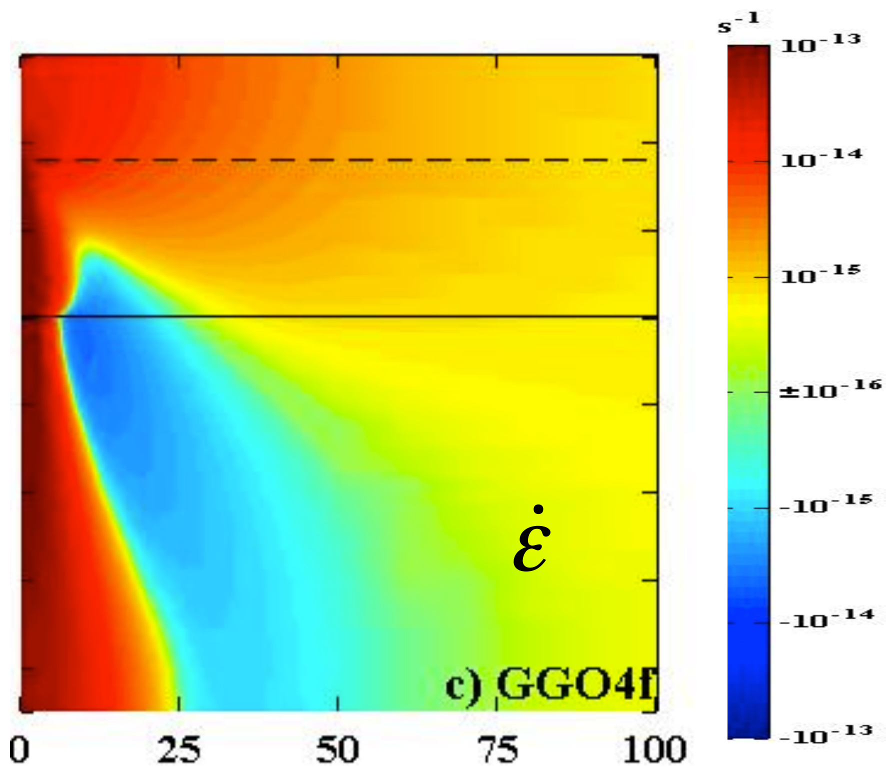

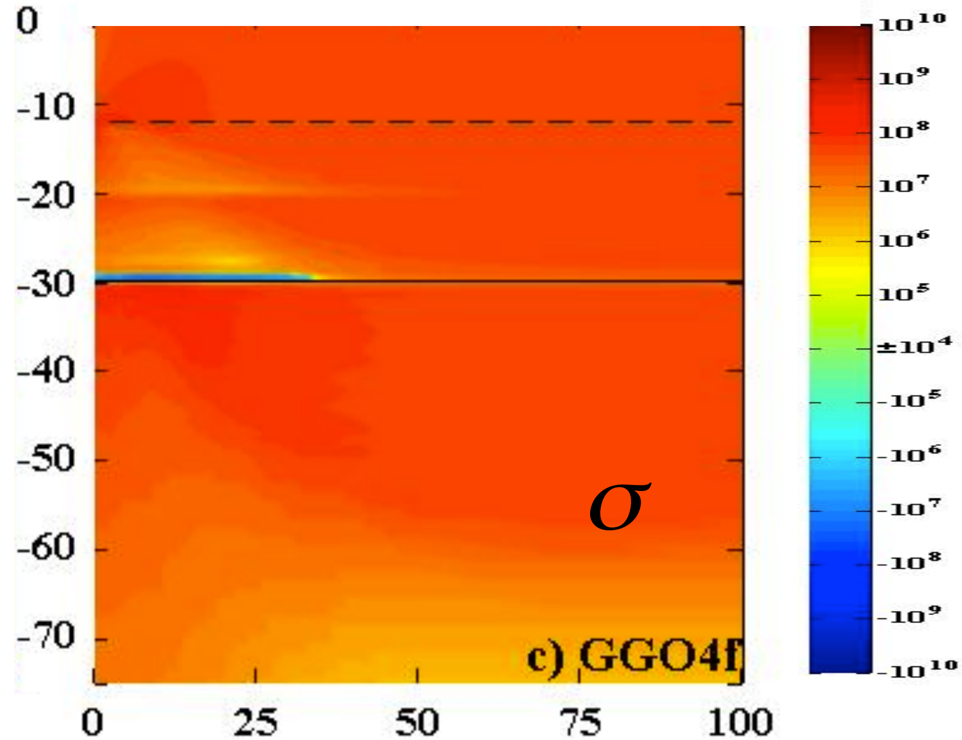

Surface velocities

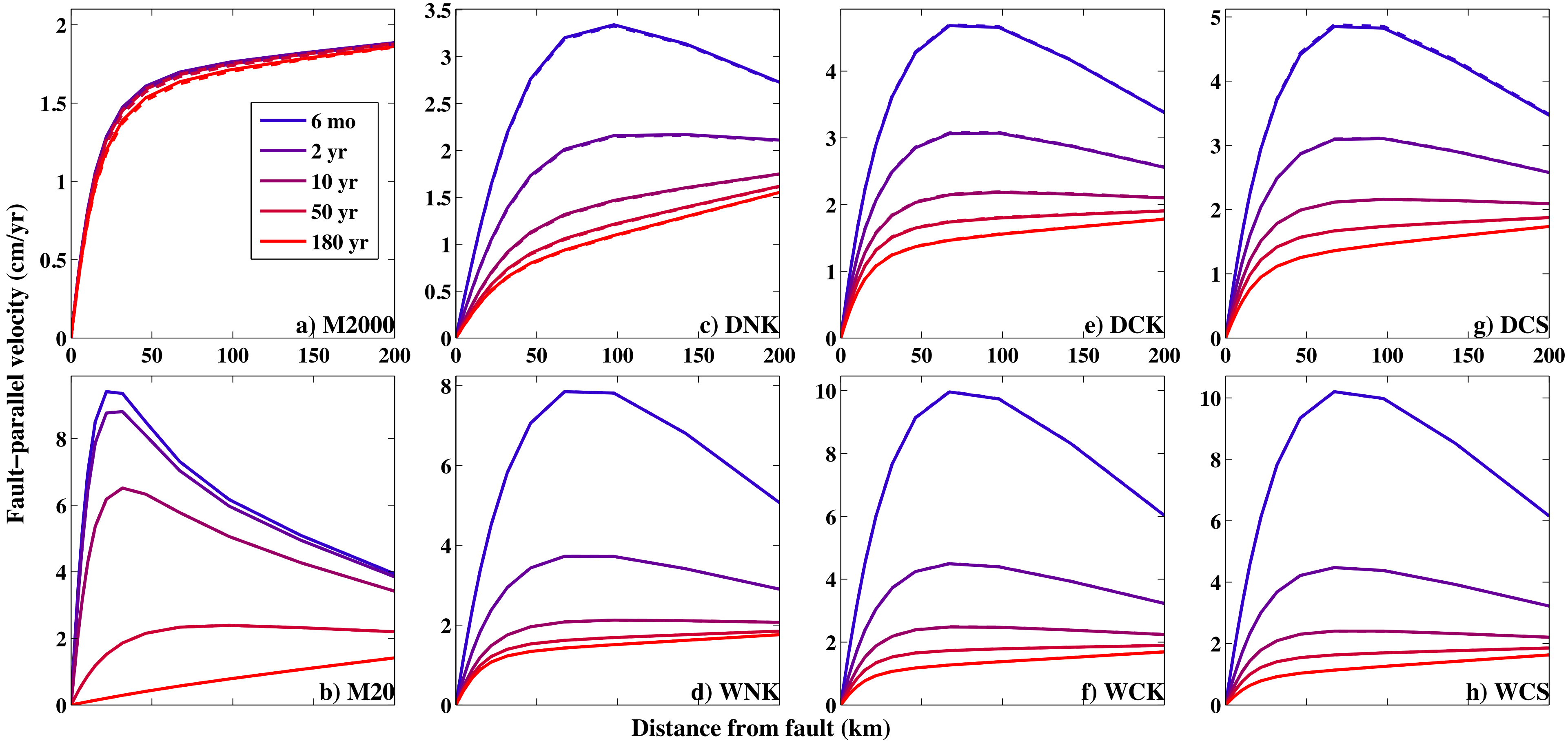

Effect of the model size

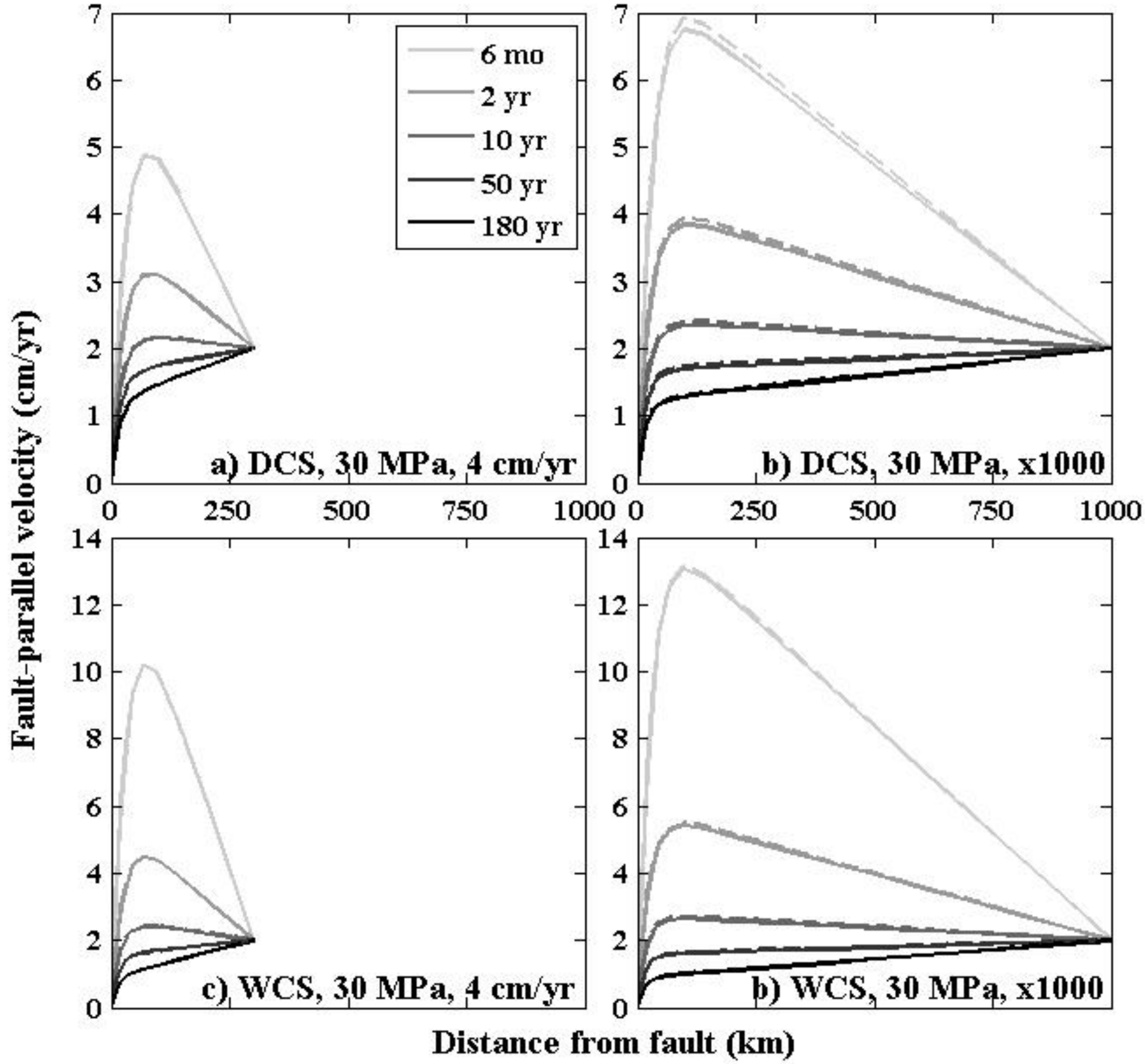

Heat flow data

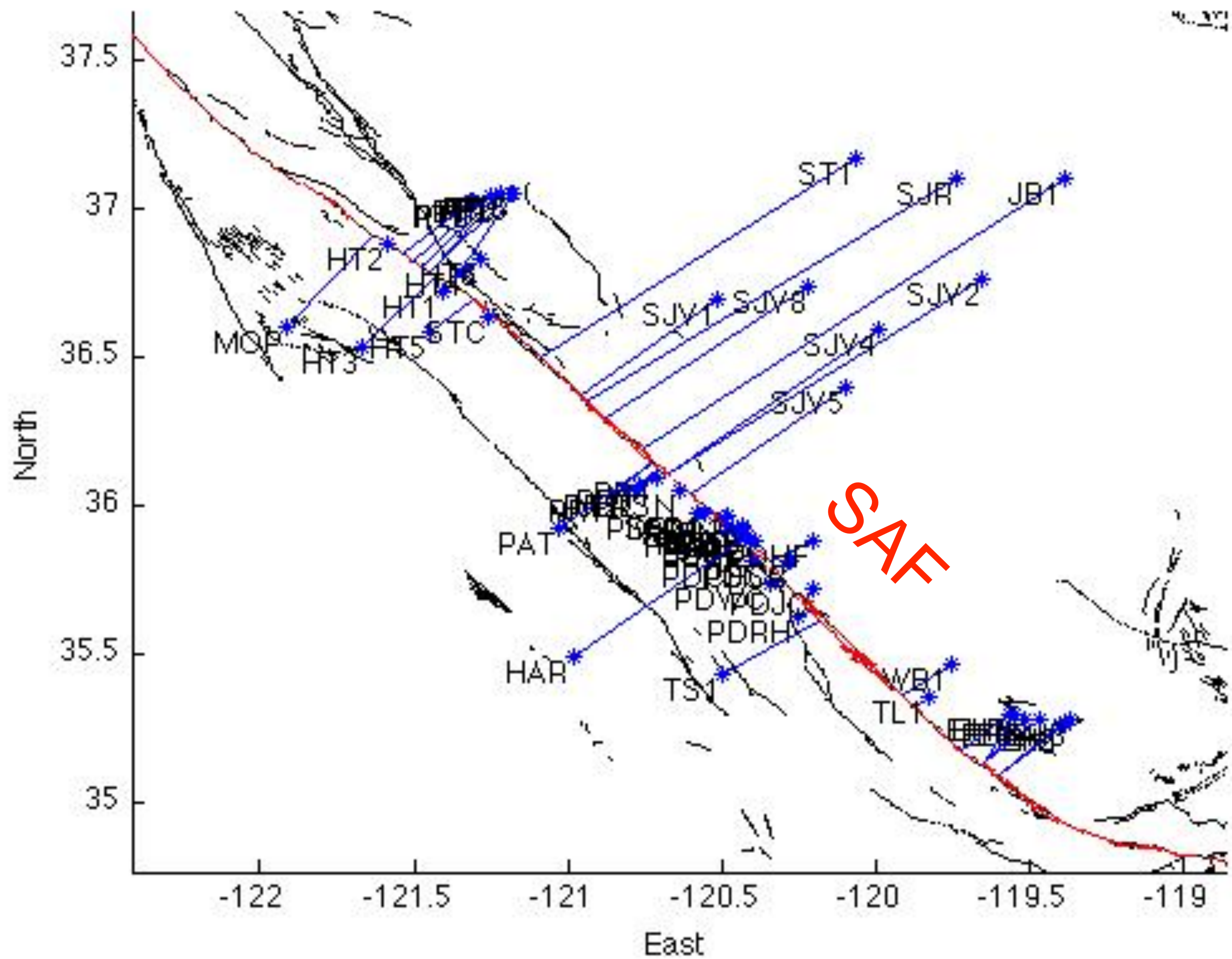

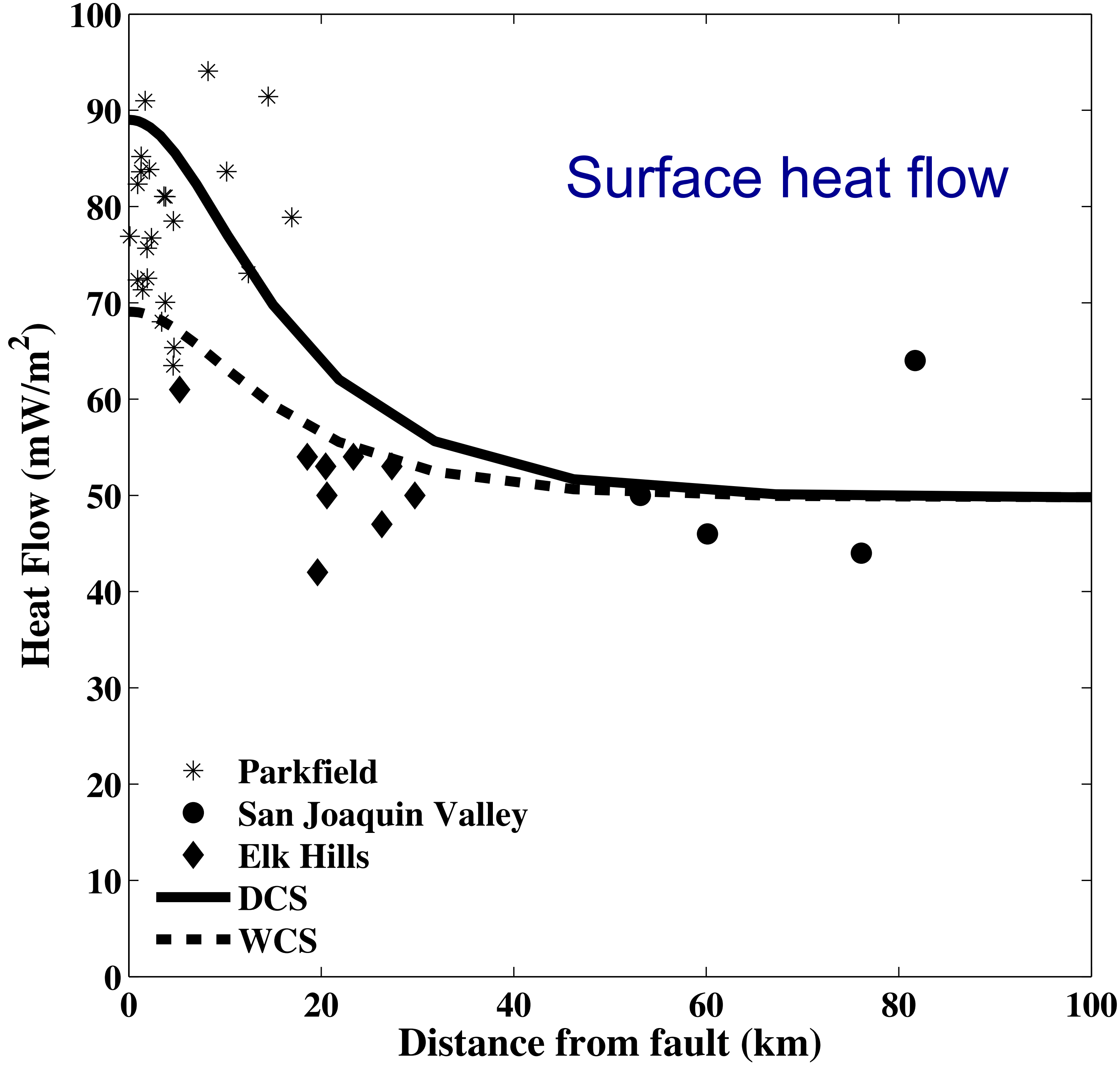
Surface heat flow
Heat Flow (mW/m^2)
Distance from fault (km)
0
10
20
30
40
50
60
70
80
90
100
0
20
40
60
80
100
Parkfield
San Joaquin Valley
Elk Hills
DCS
WCS

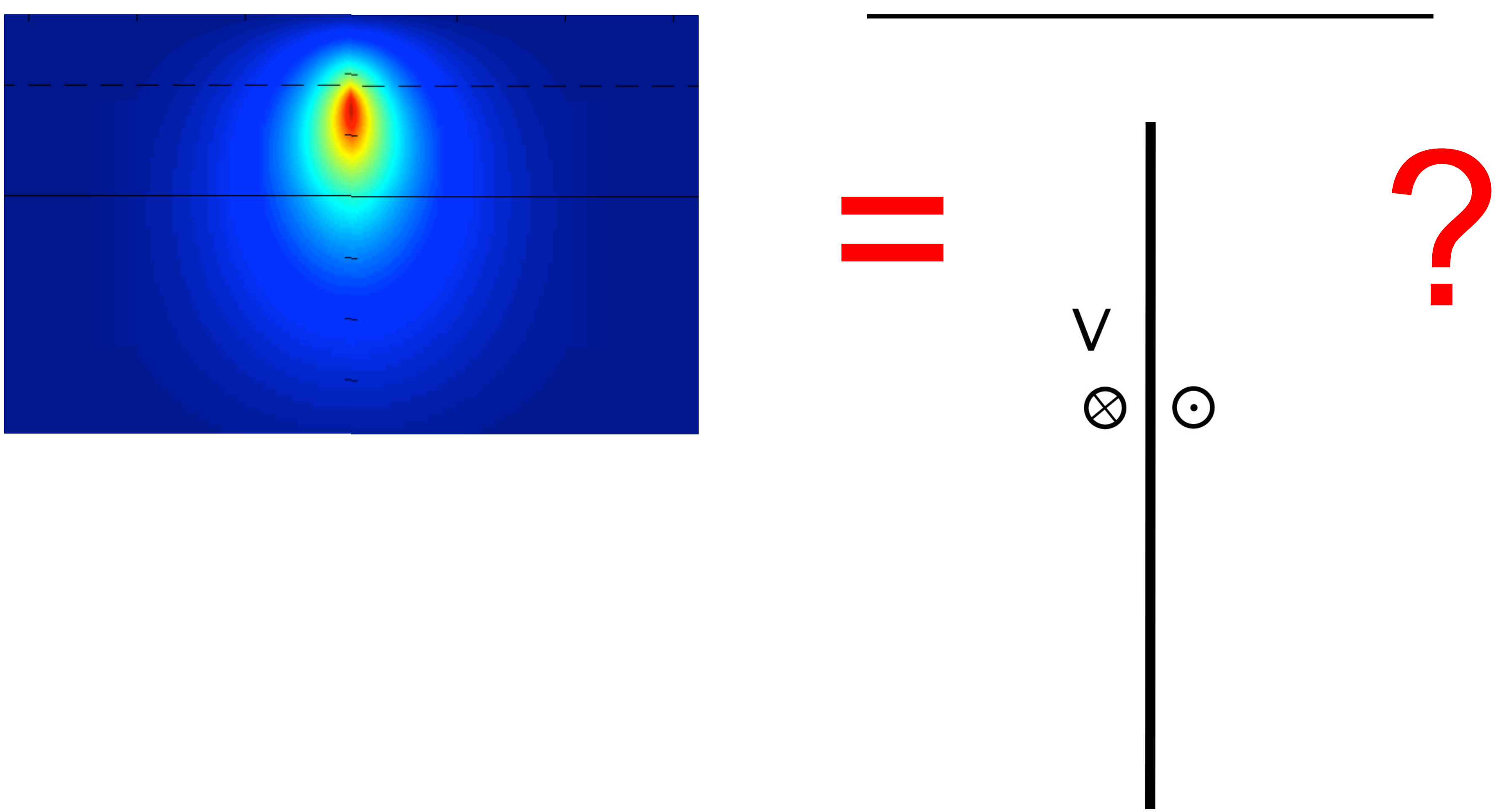
=
V
?

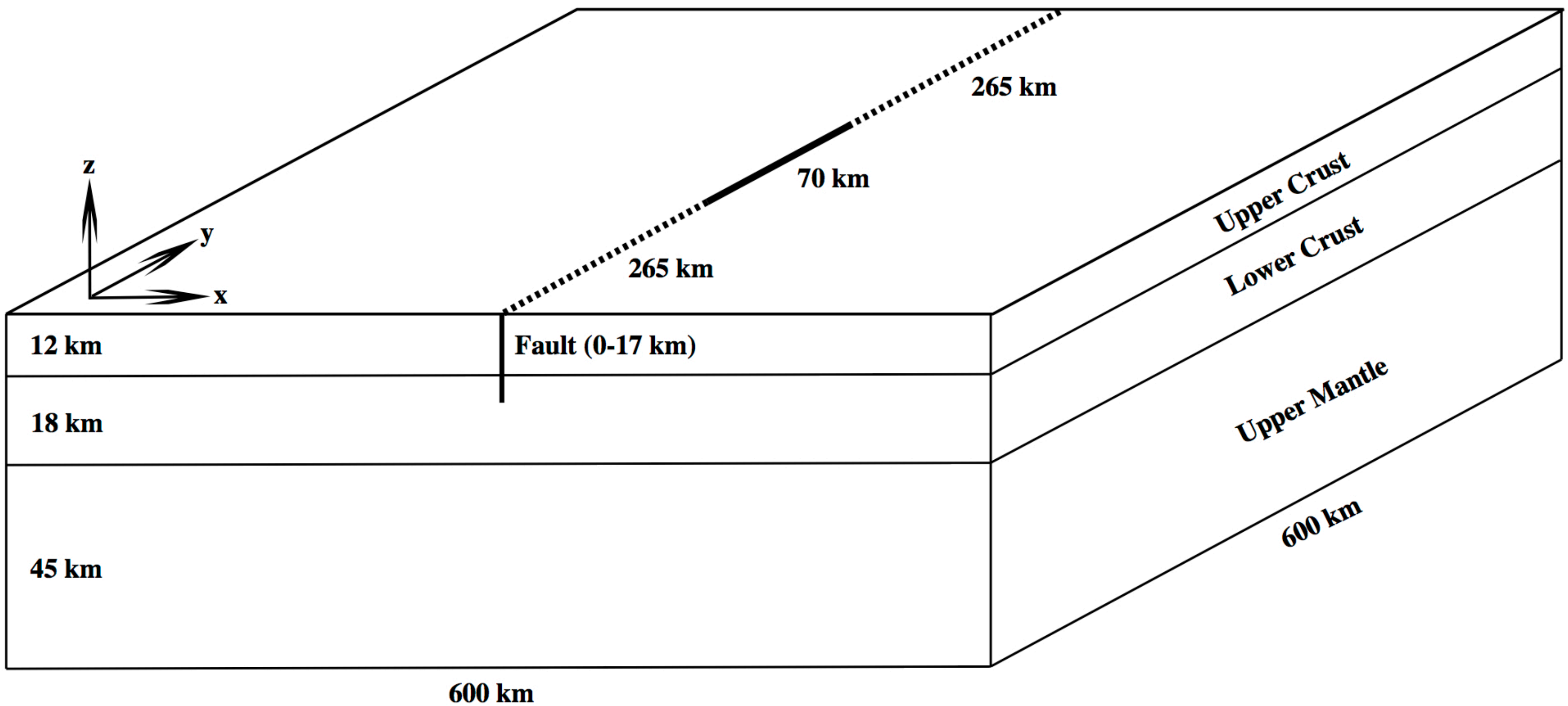

Takeuchi and Fialko, 2013

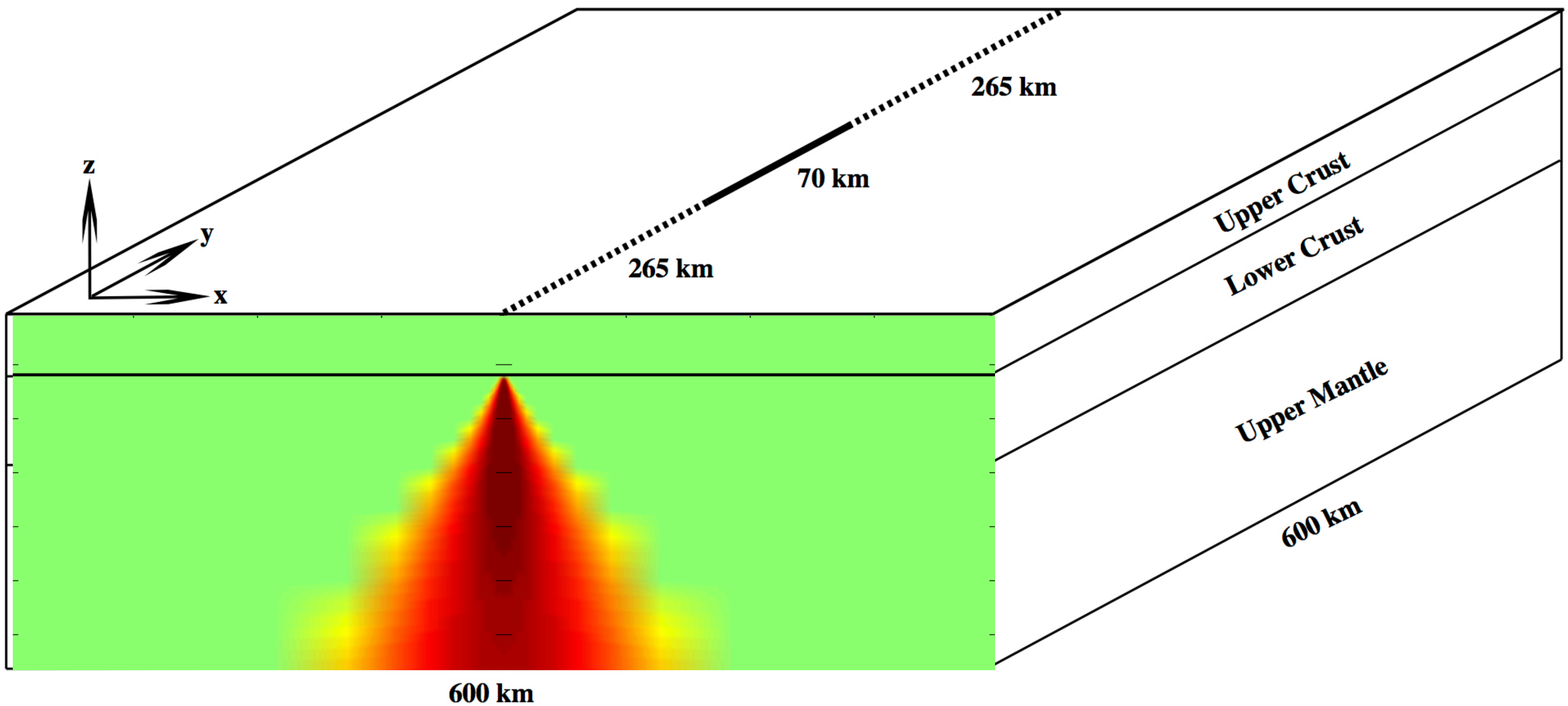

Takeuchi and Fialko, 2013

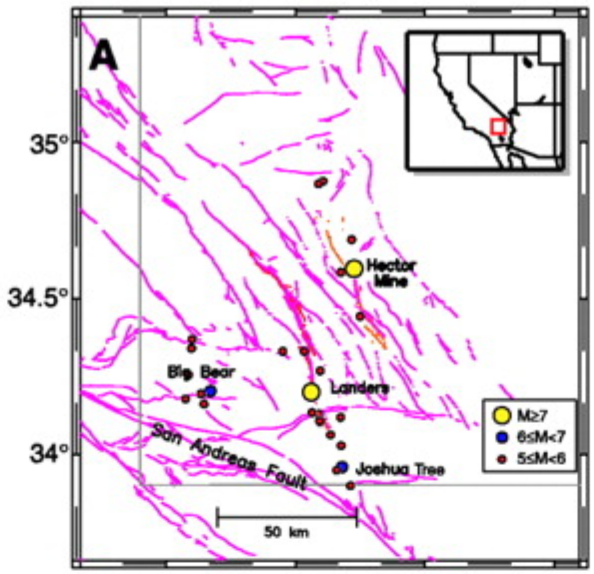

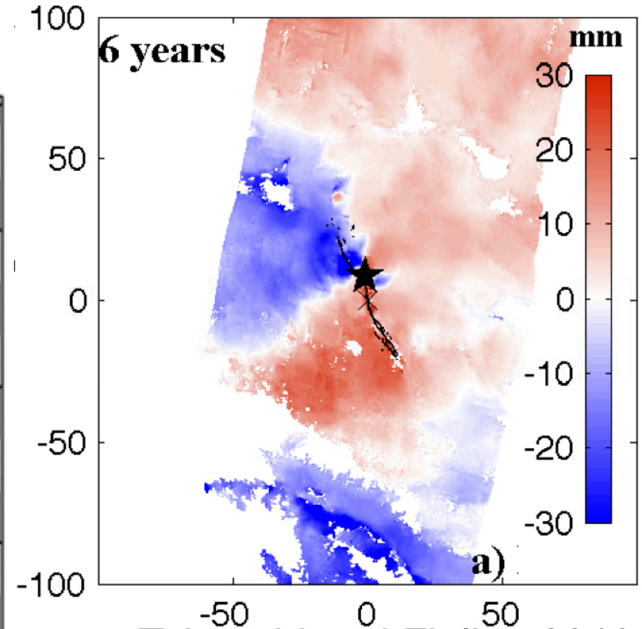

Takeuchi and Fialko, 2013

Post-seismic deformation due to the Mojave desert eqs

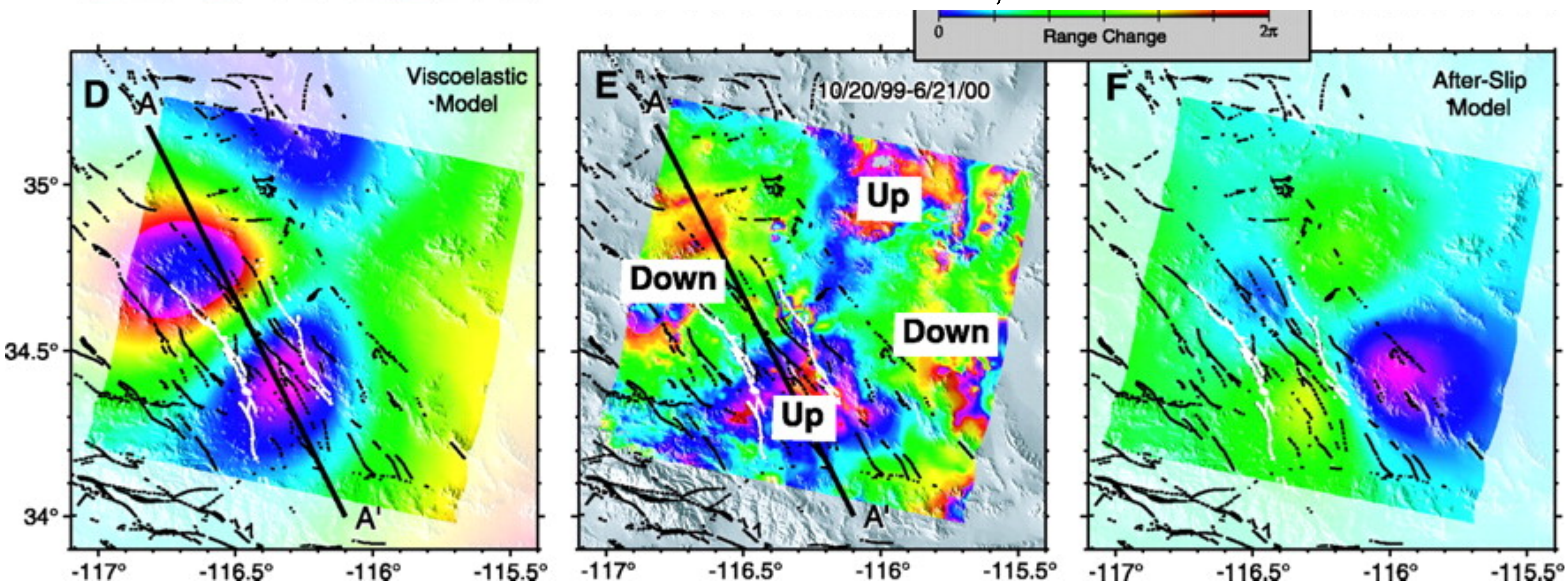

Pollitz et al., 2000; 2001

Postsesimic velocities due to a finite strike-slip fault

Afterslip / Visco-elastic relaxation

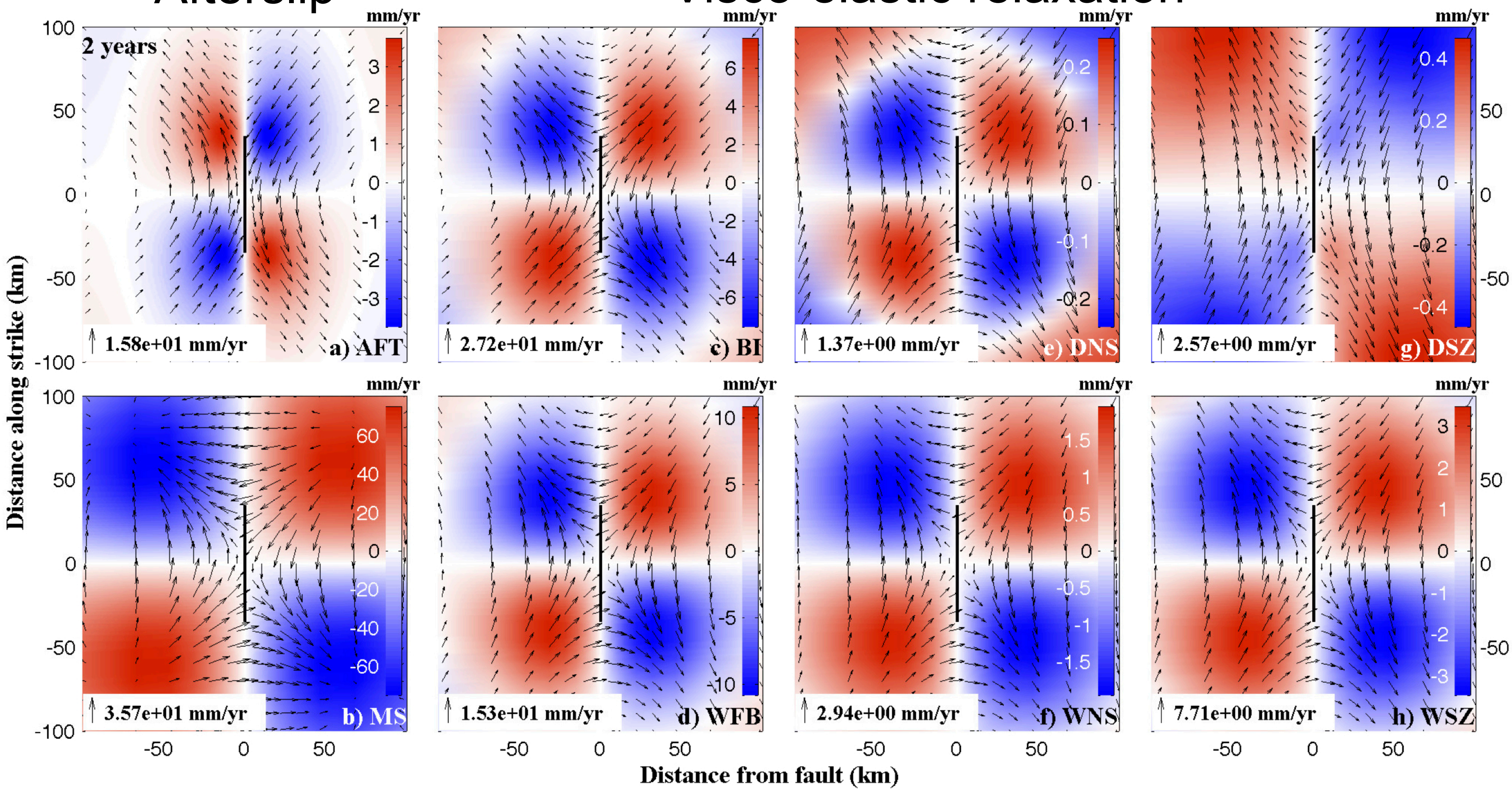

Effective viscosity after 20 Myr spin-up

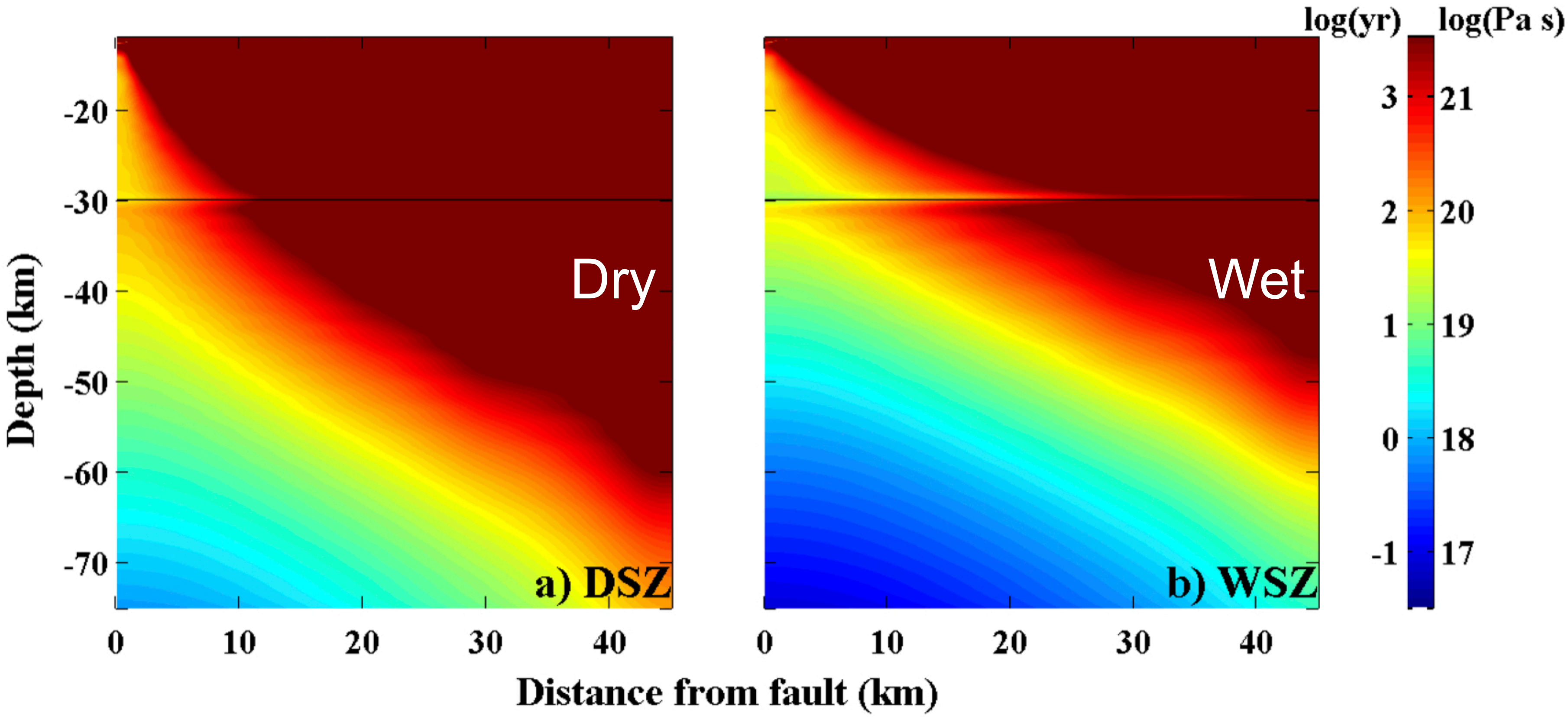

$$\eta_{eff} = \frac{\sigma}{2\dot{\varepsilon}}$$

Takeuchi and Fialko, 2013

Effective rheology

$$\dot{\varepsilon}_v = \dot{\varepsilon}_D + \dot{\varepsilon}_G = A_D \sigma^{n_D} + A_G d^{-m} \sigma^{n_G}$$

dislocation creep

diffusion creep

$n_D \sim 3$

$n_G \sim 1$

$m \sim 3$

$r \sim 1$

$$d = d_0 \sigma^{-r}$$

equilibrium grain size

ij

Assuming that the equilibrium grain size is attained when

$$R = \dot{\varepsilon}_D / \dot{\varepsilon}_G \sim O(1)$$

de Bresser et al. (1998; 2001)
Montesi and Hirth (2003)

$$\boxed{\dot{\varepsilon}_v = \left(1 + 1/R\right) A_D \left(T\right) \sigma^{n_D}}$$

Grain size evolution

$$\dot{\varepsilon}_v = \dot{\varepsilon}_D + \dot{\varepsilon}_G = A_D \sigma^{n_D} + A_G d^{-m} \sigma^{n_G}$$

dislocation creep

diffusion creep

$n_D \sim 3$

$n_G \sim 1$

$m \sim 3$

$$\dot{d}_+ = B_G p^{-1} d^{1-p} \exp\left(-\frac{H}{RT}\right)$$

static grain growth

$$\dot{d}_- = -\lambda d \dot{\varepsilon}_G$$

dynamic recrystallization

de Bresser et al. (1998; 2001)
Hall and Parmentier (2003)

Effect of dynamic recrystallization

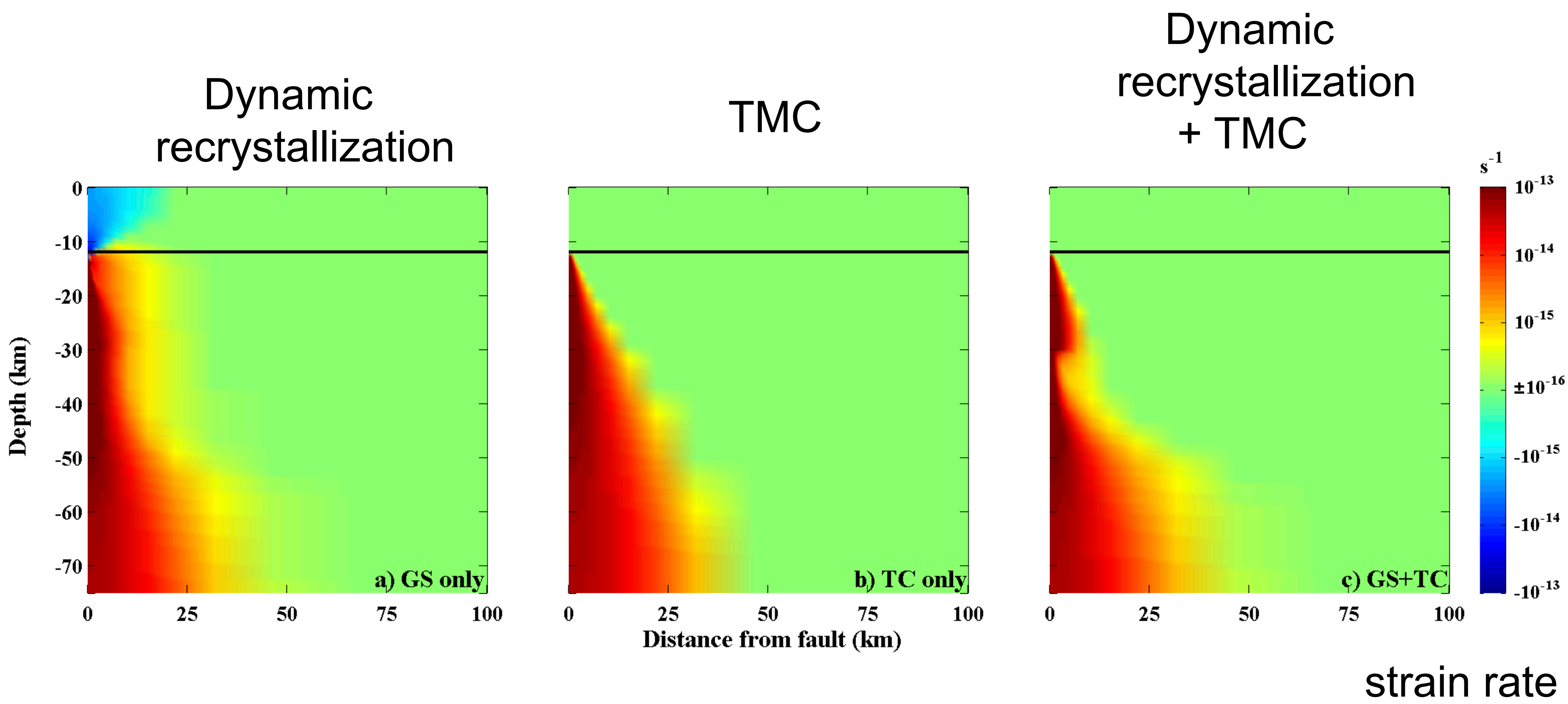

Strain localization at 20 km depth

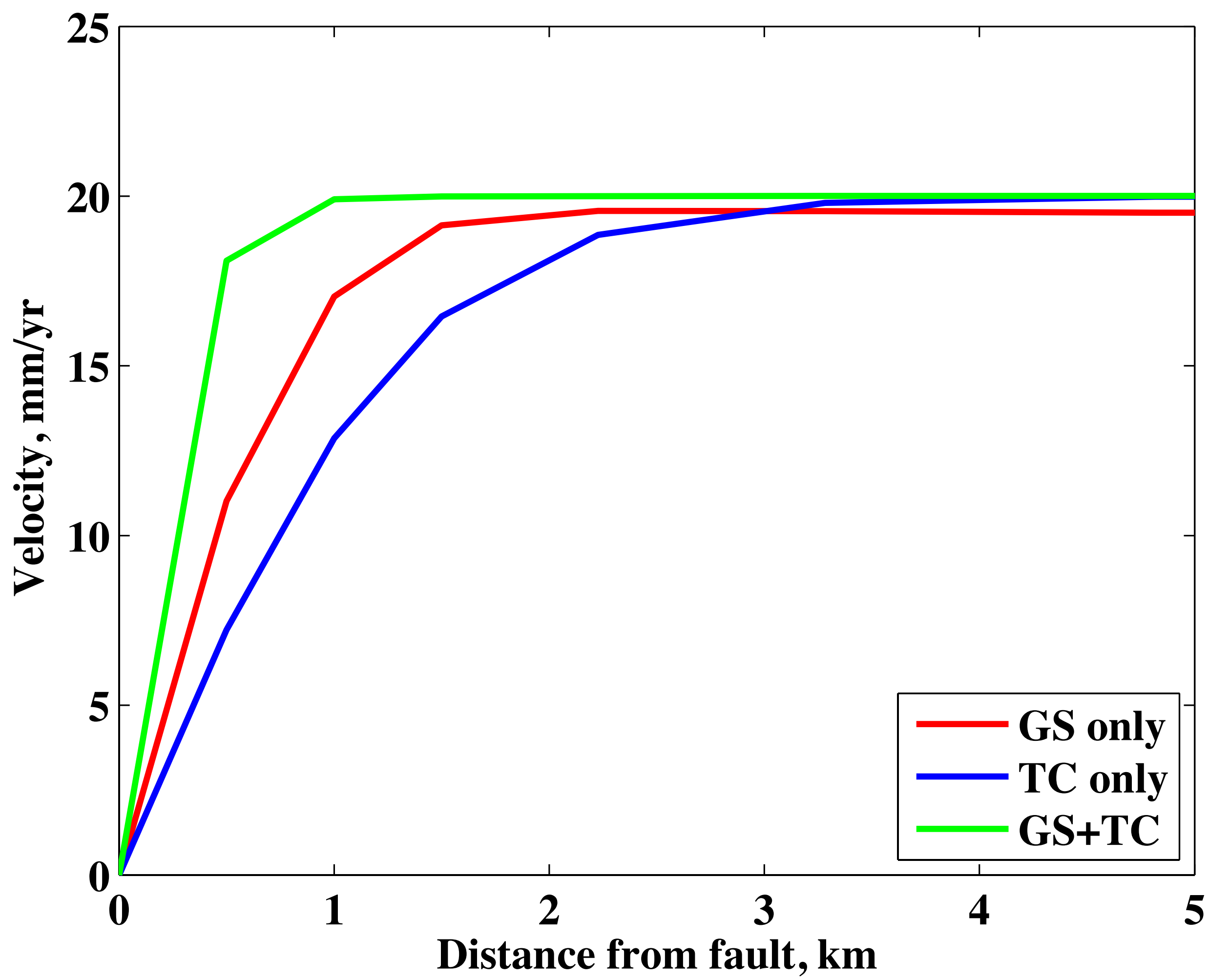

Foliation

Strain-induced separation of weak and strong mineral phases; development of anisotropic fabric

$$\dot{\varepsilon}_{tot} = \sum_{i=1}^{N} \dot{\varepsilon}_i \phi_i$$

$$\sum_{i=1}^{N} \phi_i = 1$$

Aggregate vs individual phase rheologies

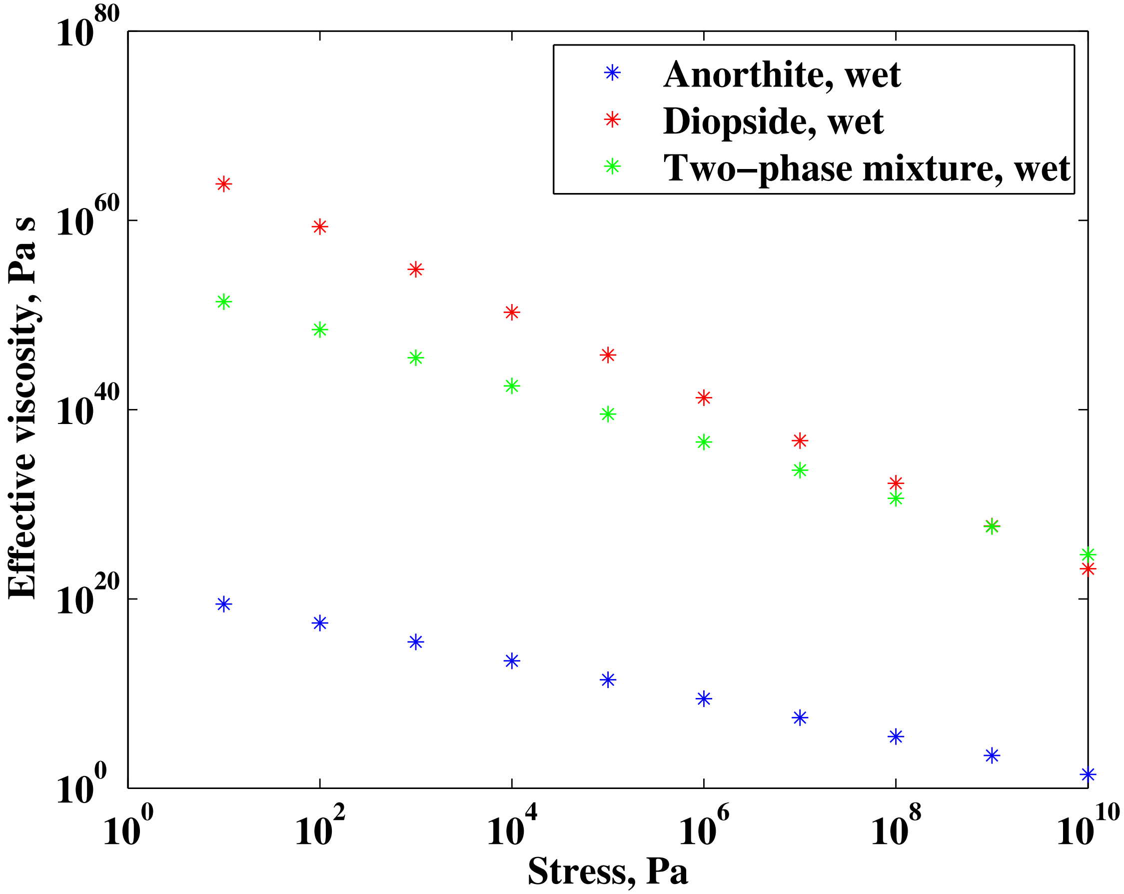

flow law parameters from Dimanov and Dresen (1995)

Deformation (and strength) is controlled by the weakest phase

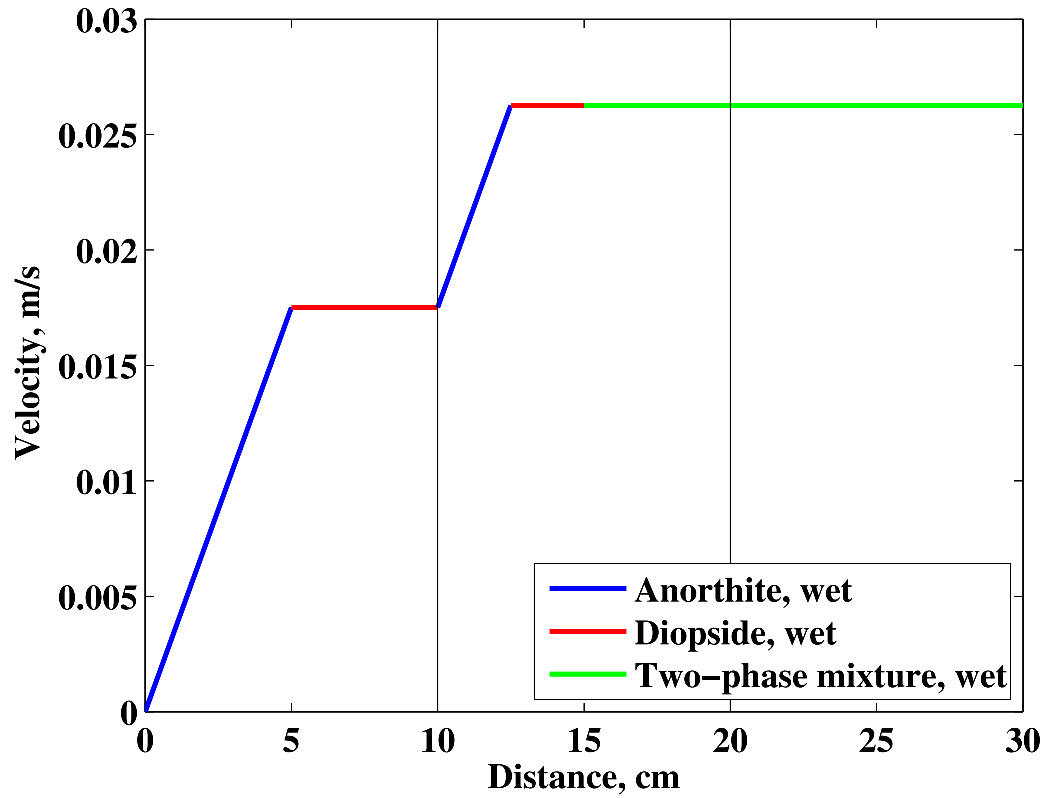

flow law parameters from Dimanov and Dresen (1995)

Where is the transition between frictional sliding and viscous flow?

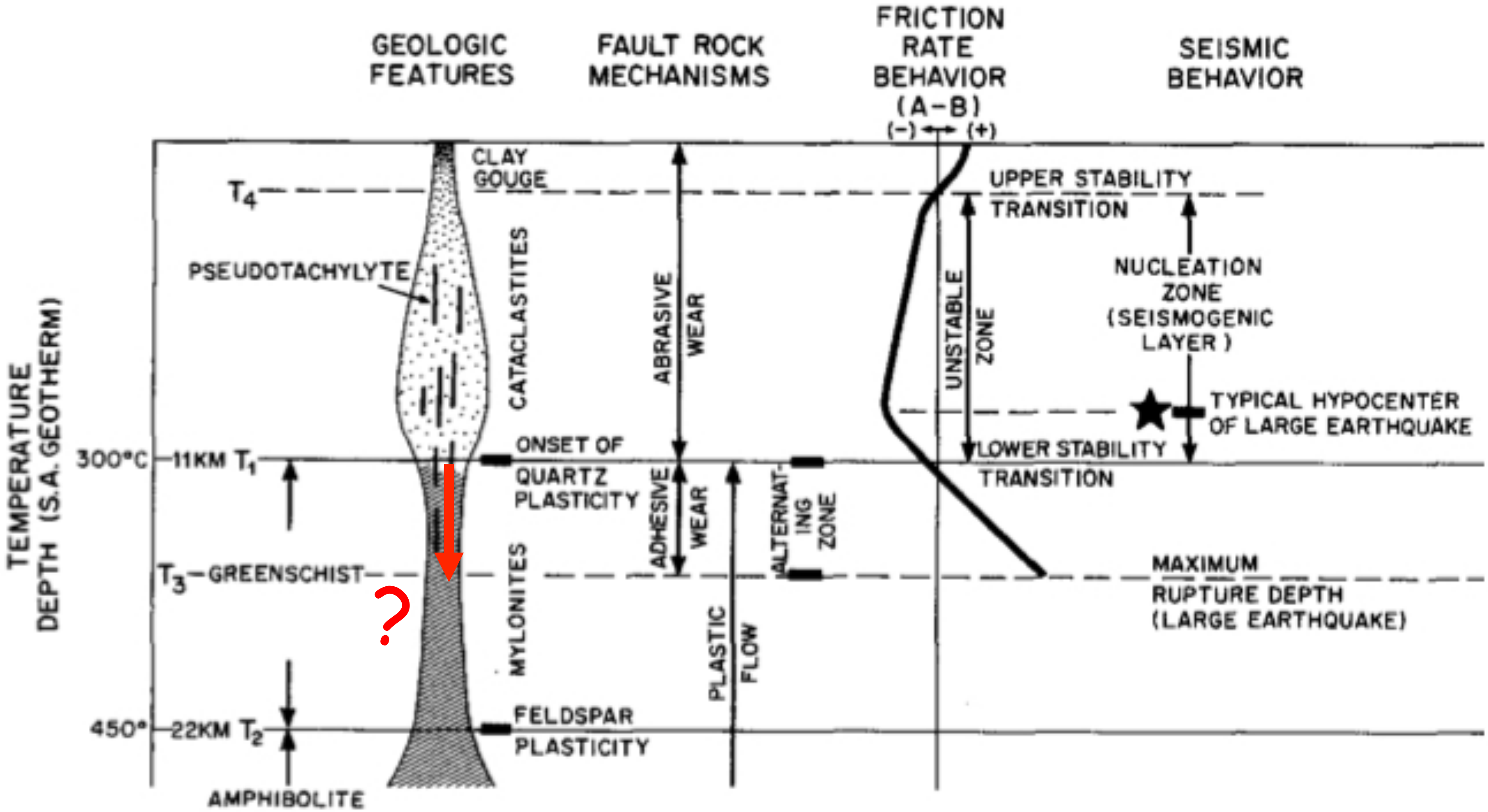

Scholz, 1988

Calico FZ tomography experiment

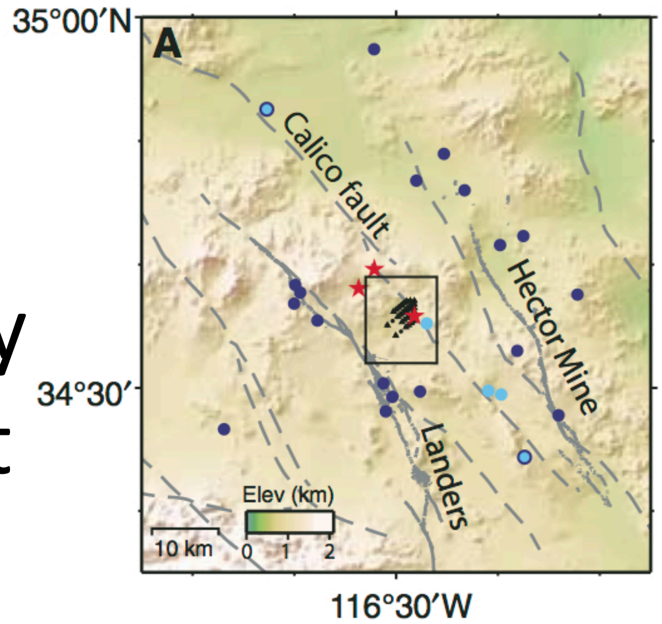

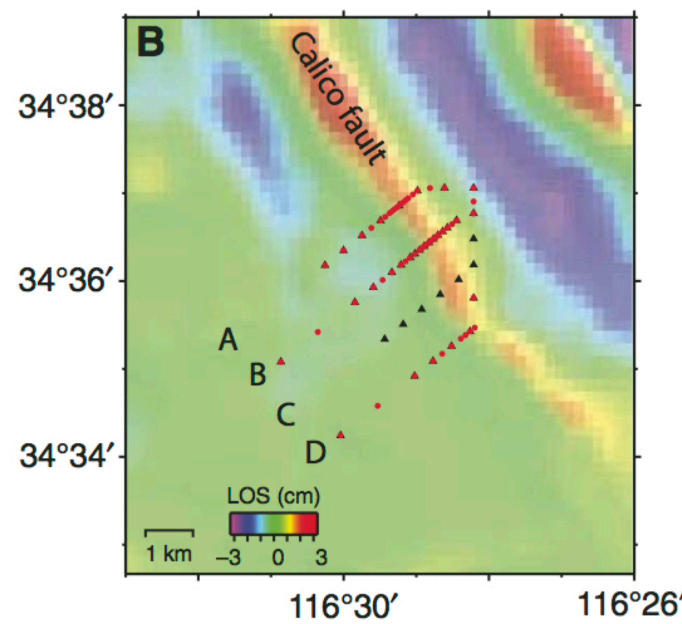

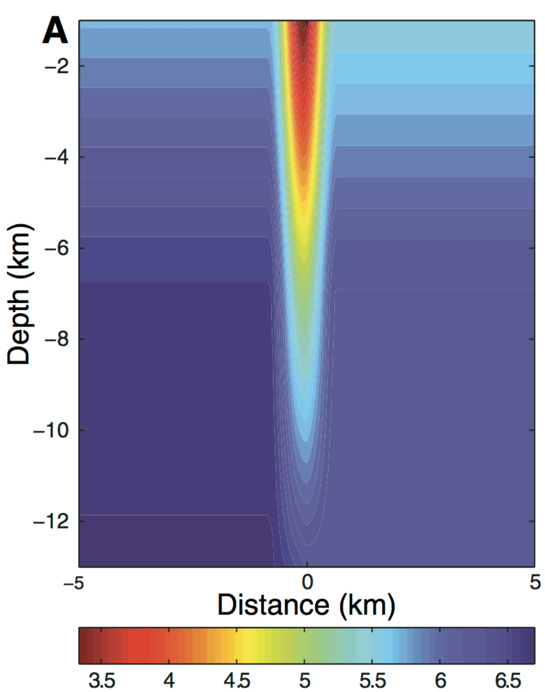

width ~ 1.5 km
G'/G ~ 50%
depth > 5 km

Cochran et al., 2009

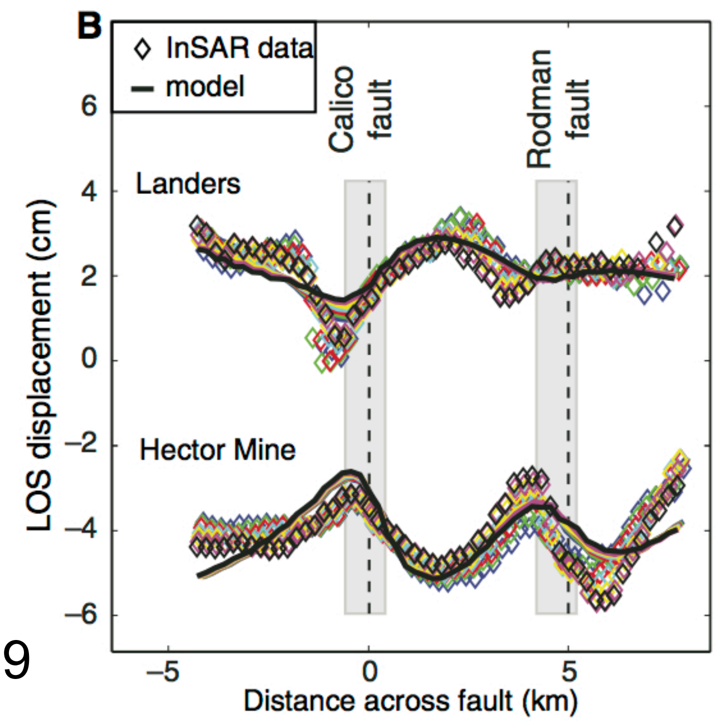

1999 M7.6 Izmit (Turkey) earthquake: "backward" displacements on nearby Mudurnu Valley and Iznik faults

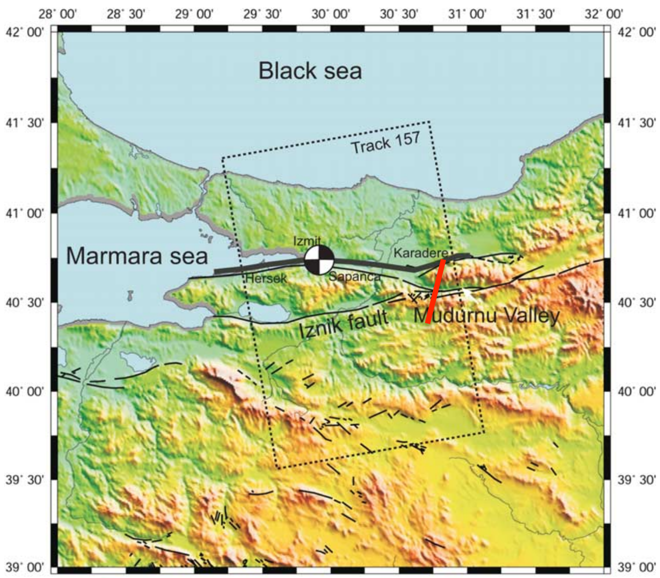

Wright et al., 2001

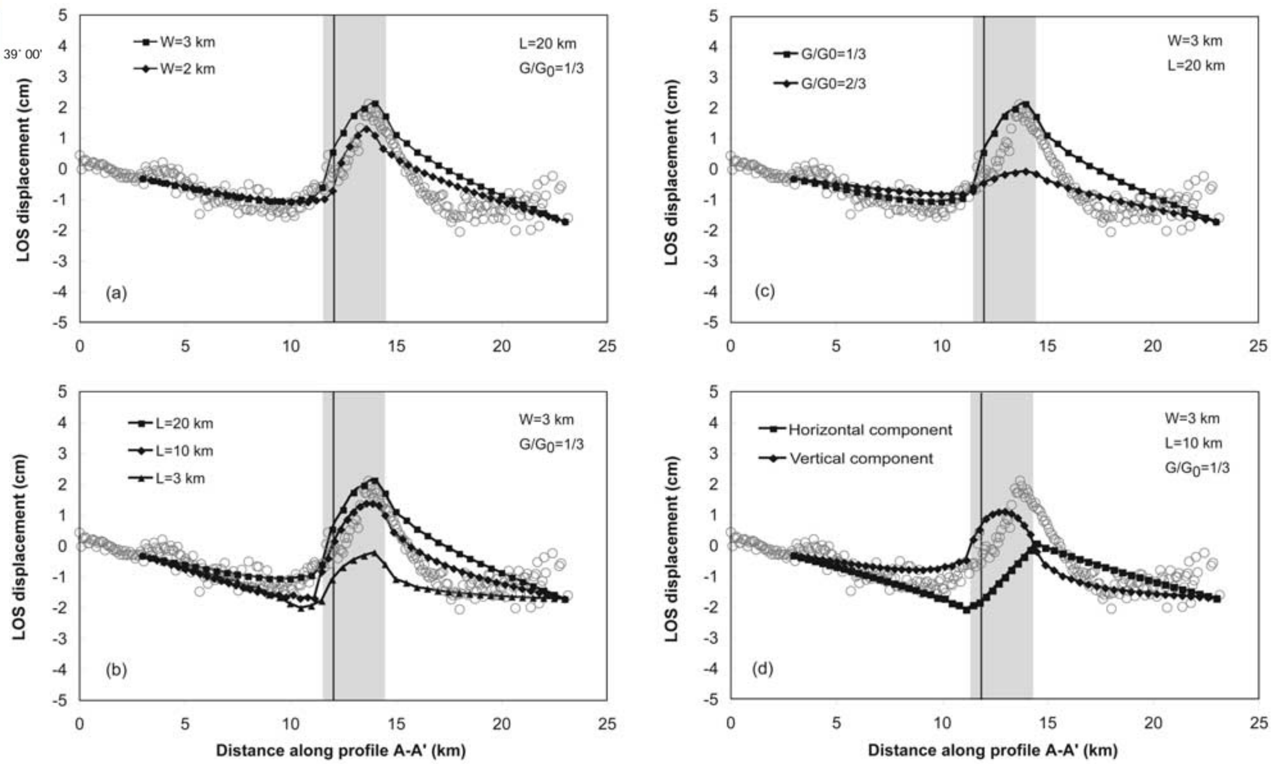

width ~ 2-3 km
G'/G ~ 30-50%
depth > 5 km

Hamiel and Fialko, 2007

San Jacinto: compliant fault zone

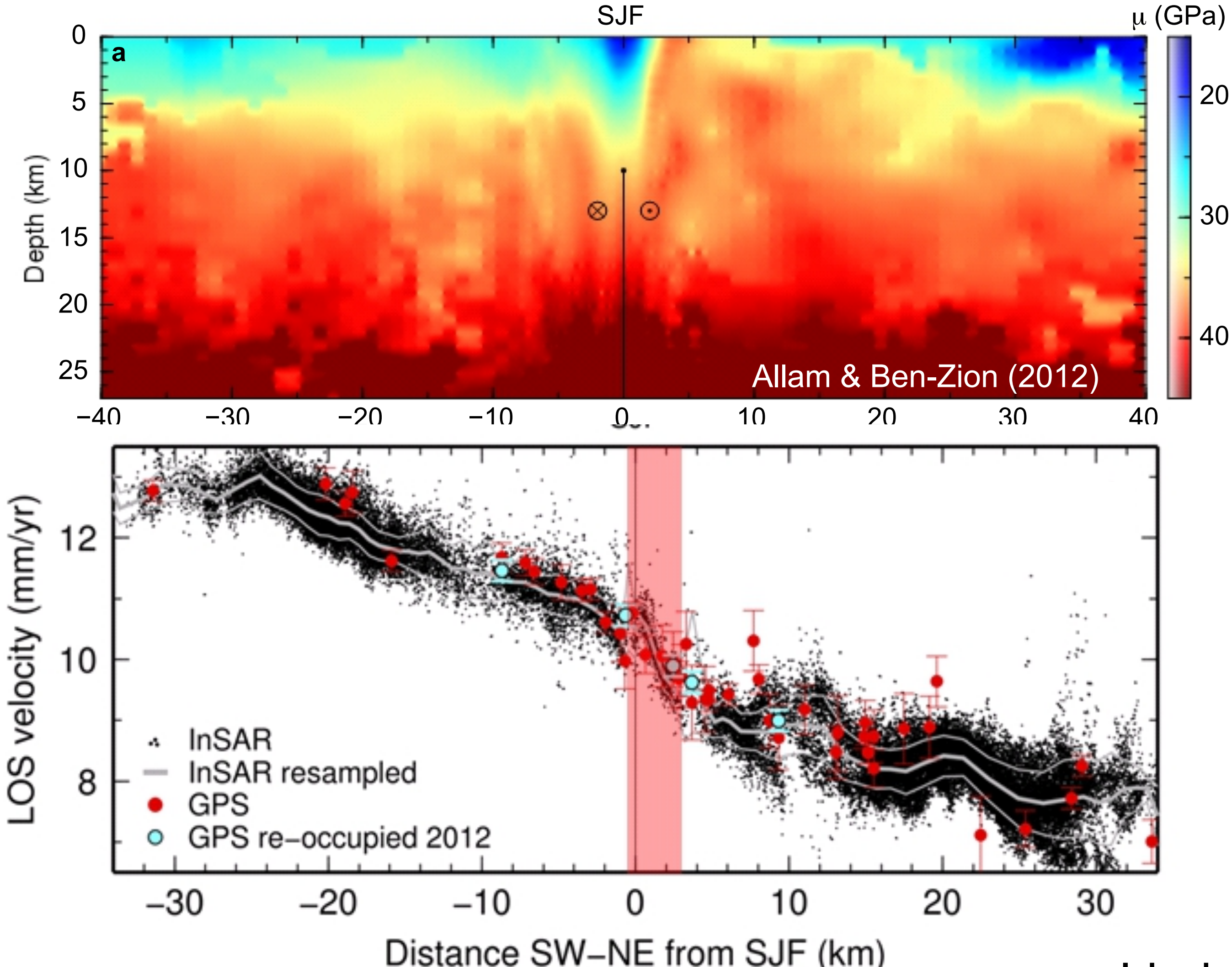

- Increases local strain rate by 40 - 50%

Lindsey et al., I2013

Southern San Andreas: localized vs distributed surface creep

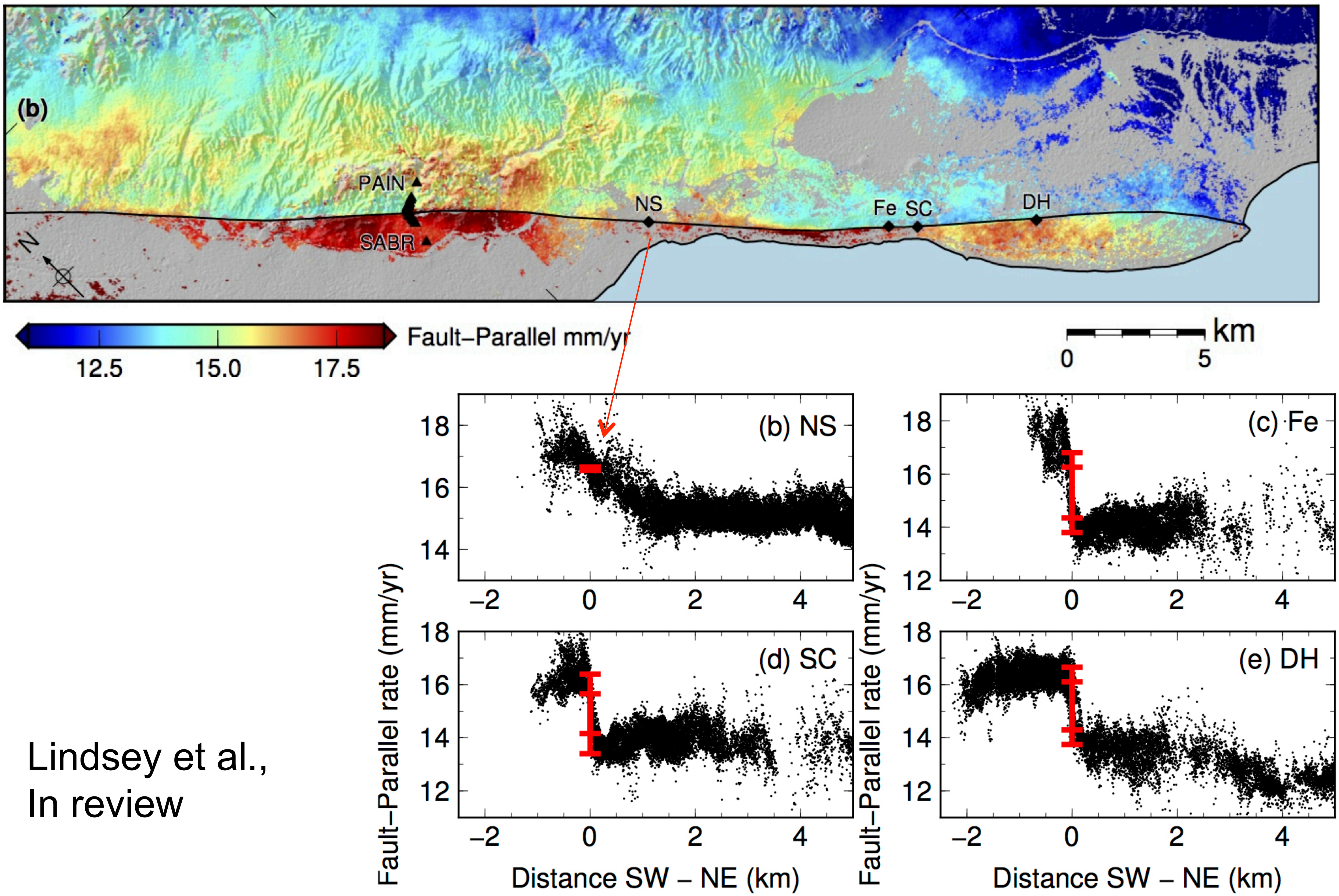

Lindsey et al.,
In review

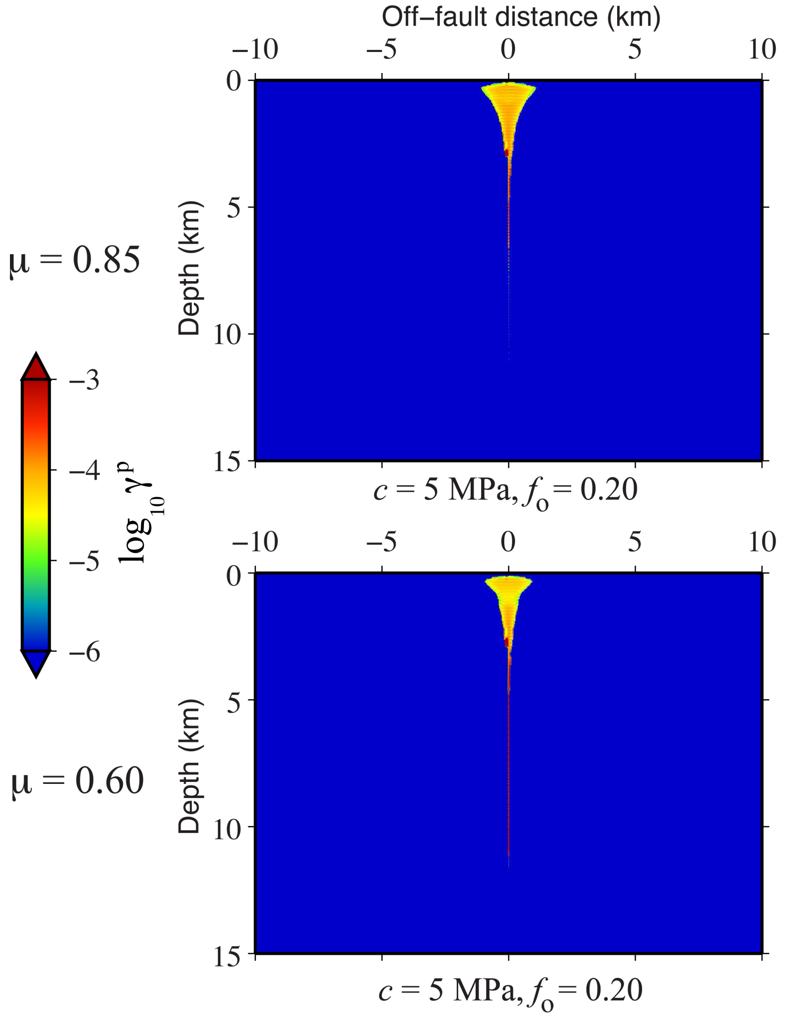

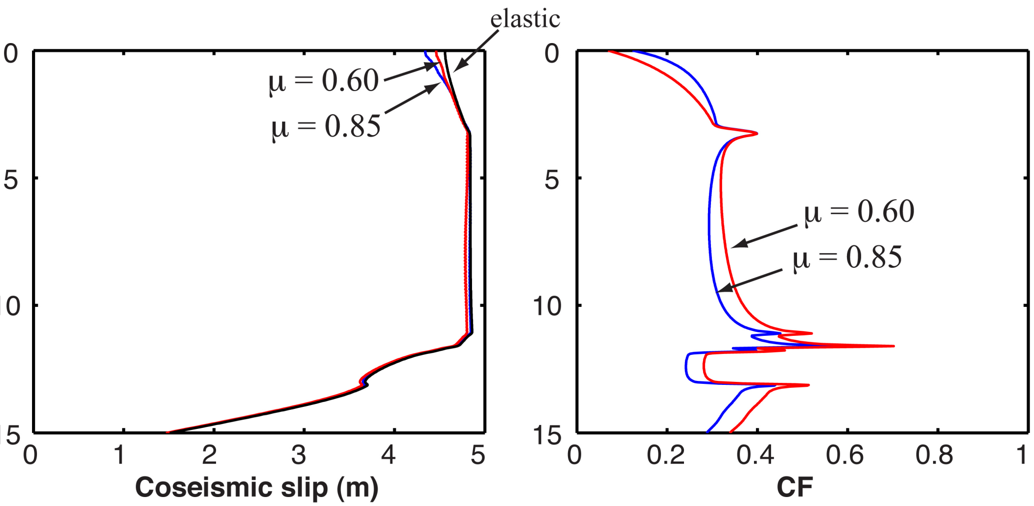

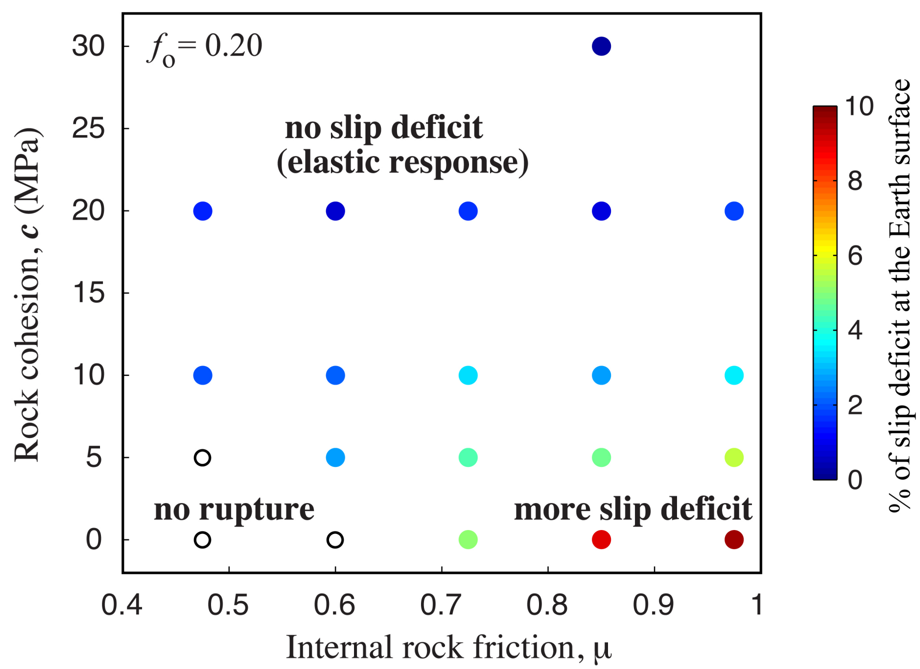

distribution of plastic strain

Kaneko and Fialko, l2011

Fault zone architecture

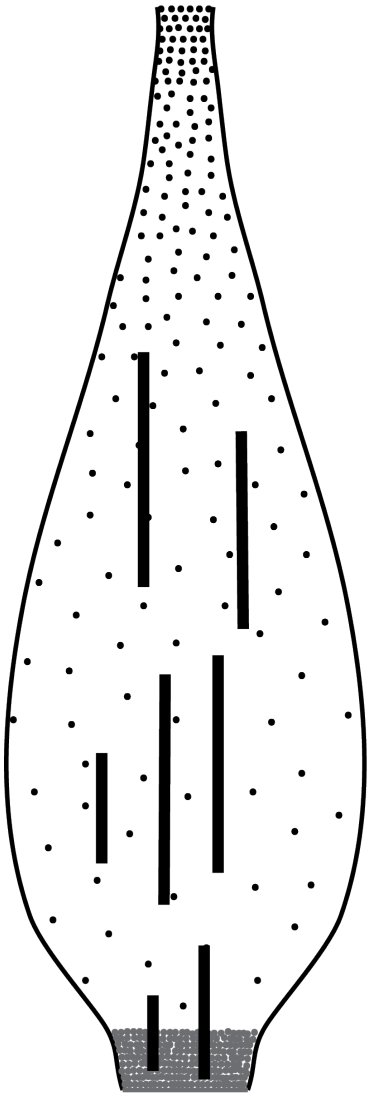

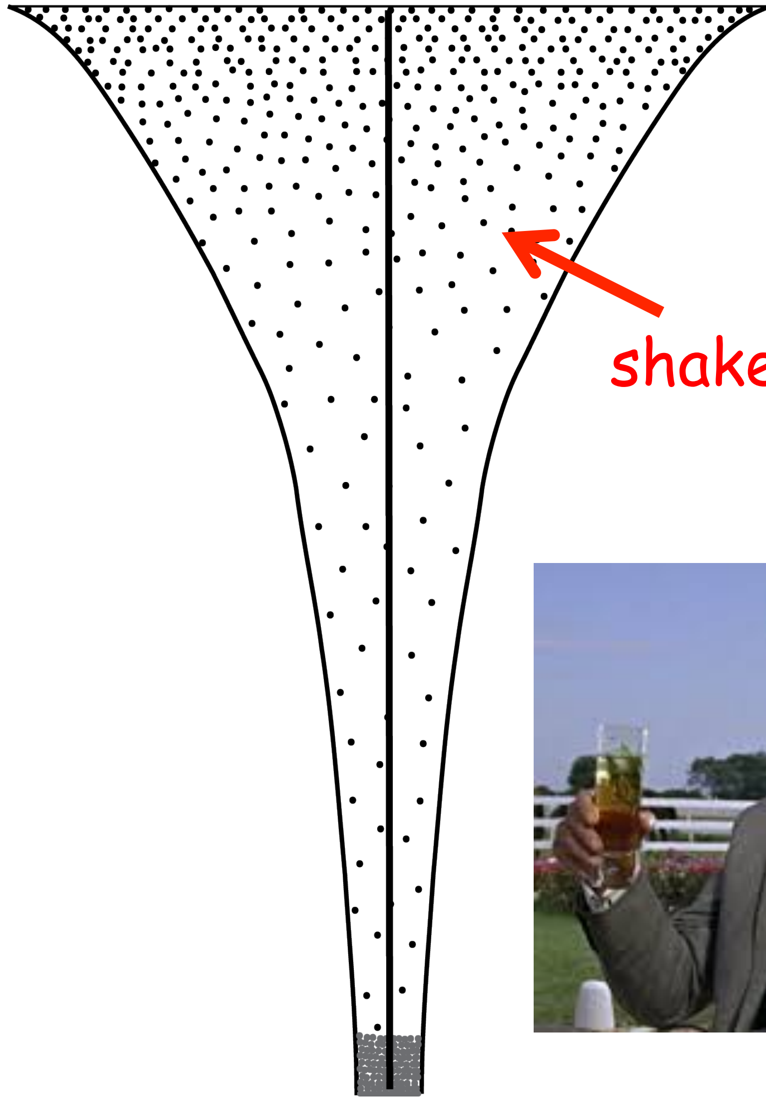

shaken, not stirred

Scholz, 1988; 2002

Conclusions

- Lab-derived rheologies give rise to permanent localization of strain in deep “roots” of major strike-slip faults
- The shear zone width in the ductile substrate inversely depends on the fault slip rate and the effective viscosity of the substrate
- Ductile strength of the lithosphere is of the order of ~50 MPa, only weakly dependent on composition, water content, and geotherm – in good agreement with petrologic data
- Thermally weakened shear zones (result of thermomechanical coupling) have little effect on postseismic deformation